



## LJMU Research Online

**Spear, JK, Grabowski, M, Sekhavati, Y, Costa, CE, Goldstein, DM, Petrullo, LA, Peterson, AL, Lee, AB, Shattuck, MR, Gómez-Olivencia, A and Williams, SA**

**Evolution of vertebral numbers in primates, with a focus on hominoids and the last common ancestor of hominins and panins**

<http://researchonline.ljmu.ac.uk/id/eprint/22821/>

### Article

**Citation** (please note it is advisable to refer to the publisher's version if you intend to cite from this work)

**Spear, JK, Grabowski, M, Sekhavati, Y, Costa, CE, Goldstein, DM, Petrullo, LA, Peterson, AL, Lee, AB, Shattuck, MR, Gómez-Olivencia, A and Williams, SA (2023) Evolution of vertebral numbers in primates, with a focus on hominoids and the last common ancestor of hominins and panins. Journal**

LJMU has developed [LJMU Research Online](#) for users to access the research output of the University more effectively. Copyright © and Moral Rights for the papers on this site are retained by the individual authors and/or other copyright owners. Users may download and/or print one copy of any article(s) in LJMU Research Online to facilitate their private study or for non-commercial research. You may not engage in further distribution of the material or use it for any profit-making activities or any commercial gain.

The version presented here may differ from the published version or from the version of the record. Please see the repository URL above for details on accessing the published version and note that access may require a subscription.

For more information please contact [researchonline@ljmu.ac.uk](mailto:researchonline@ljmu.ac.uk)

<http://researchonline.ljmu.ac.uk/>

1 **Evolution of vertebral numbers in primates, with a focus on hominoids and the last common**  
2 **ancestor of hominins and panins**

3  
4 **Abstract**

5 The primate vertebral column has been studied extensively, with a particular focus on hominoid primates  
6 and the last common ancestor of humans and chimpanzees. The number of vertebrae in hominoids—up  
7 to and including the last common ancestor of humans and chimpanzees—is subject to considerable  
8 debate. However, few formal ancestral state reconstructions exist, and none include a broad sample of  
9 primates or account for the correlated evolution of the vertebral column. Here, we conduct an ancestral  
10 state reconstruction using a model of evolution that accounts for both homeotic (changes of one type of  
11 vertebra to another) and meristic (addition or loss of a vertebra) change. Our results suggest that  
12 ancestral primates were characterized by 29 precaudal vertebrae, with the most common formula being  
13 seven cervical, 13 thoracic, six lumbar, and three sacral vertebrae. Extant hominoids evolved tail loss  
14 and a reduced lumbar column via sacralization (homeotic transition at the last lumbar vertebra). Our  
15 results indicate that the ancestral hylobatid had seven cervical, 13 thoracic, five lumbar, and four sacral  
16 vertebrae and the ancestral hominid had seven cervical, 13 thoracic, four lumbar, and five sacral  
17 vertebrae. The last common ancestor of humans and chimpanzees likely either retained this ancestral  
18 hominid formula or was characterized by an additional sacral vertebra, possibly acquired through a  
19 homeotic shift at the sacrococcygeal border. Our results support the ‘short-back’ model of hominin  
20 vertebral evolution, which postulates that hominins evolved from an ancestor with an African ape-like  
21 numerical composition of the vertebral column.

22  
23 **Keywords:** Vertebral column; Last common ancestor; Hominin evolution; Bipedalism; Ancestral state  
24 reconstruction

## 26 **1. Introduction**

27           The numerical composition of the vertebral column and its evolution has been of interest to  
28 natural historians and other biologists for centuries. Modern understanding of evolutionary processes  
29 and the underlying developmental genetics of vertebra segmentation and specification, coupled with  
30 increasing phylogenetic resolution, permits research into the conservation and complexity of vertebral  
31 numbers among mammals. Numbers of cervical vertebrae are essentially fixed at seven in the vast  
32 majority of mammals (Galis, 1999a), and presacral number (combined cervical, thoracic, and lumbar) is  
33 also fairly constrained, at least in certain lineages (Narita and Kuratani, 2005; Galis et al., 2014;  
34 Williams et al., 2019b). Mammals that engage in suspensory behavior often depart from and are more  
35 variable in presacral numbers of vertebrae than their non-suspensory close relatives (Williams et al.,  
36 2019b). One such group is hominoids (apes and humans), and interpretations of the evolutionary history  
37 of both suspensory positional behavior and vertebral numbers in this group is contentious (Latimer and  
38 Ward, 1993; Haeusler et al., 2002; Pilbeam, 2004; Rosenman, 2008; Lovejoy et al., 2009; Lovejoy and  
39 McCollum, 2010; McCollum et al., 2010; Williams, 2012a; Machnicki et al., 2016a; Williams et al.,  
40 2016, 2019a; Thompson and Almécija, 2017; Tardieu and Haeusler, 2019; Machnicki and Reno, 2020;  
41 Williams and Pilbeam, 2021), in large part due to its implications for the ancestral condition from which  
42 hominins evolved bipedal locomotion.

43           There are currently three models that hypothesize the numbers of vertebrae characterizing the  
44 last common ancestor (LCA) of hominins (members of the human lineage) and panins (chimpanzees and  
45 bonobos;  $LCA_{H-P}$ ). These focus on the number of lumbar vertebrae, which is the presumed target of  
46 selection due to its role in vertical posture and lordosis, and the dorsal concavity of the lumbar spine  
47 (Lovejoy, 2005; Whitcome et al., 2007; Williams et al., 2022). The ‘long back’ model (Fig. 1A) posits  
48 that the  $LCA_{H-P}$  maintained six lumbar vertebrae as well as a long thoracic column consisting of 13  
49 elements (Lovejoy et al., 2009; Lovejoy and McCollum, 2010; McCollum et al., 2010; Machnicki and  
50 Reno, 2020), together contributing to a 26-element presacral column. The ‘intermediate back’ model

51 suggests that the LCA<sub>H-P</sub> was characterized by five lumbar vertebrae and either 12 or 13 thoracic  
52 vertebrae (Johanson et al., 1982; Haeusler et al., 2002; Machnicki et al., 2016a; Tardieu and Haeusler,  
53 2019), totaling either 24 or 25 presacral vertebrae (Fig. 1B). The ‘short back’ model posits that the  
54 LCA<sub>H-P</sub> possessed four lumbar vertebrae and 13 thoracic vertebrae (Pilbeam, 2004; Williams, 2012a;  
55 Williams et al., 2016, 2019a; Williams and Pilbeam, 2021), yielding a short presacral column consisting  
56 of 24 elements (Fig 1C).

57         Among extant taxa, many non-hominoid primates are characterized by a vertebral formula  
58 consisting of seven cervical (C), 13 thoracic (T), and six lumbar (L) vertebrae, including many  
59 platyrrhine and cercopithecoid monkeys, and this presacral combination was proposed as ancestral for  
60 primates, anthropoids, or catarrhines (Schultz and Straus, 1945; Pilbeam, 2004; Williams, 2011, 2012a).  
61 Extant African apes, specifically western gorillas (*Gorilla gorilla*) and both chimpanzees (*Pan*  
62 *troglydites*) and bonobos (*Pan paniscus*), are characterized by 7C, 13T, and 4L modally, while eastern  
63 gorillas (*Gorilla beringei*) have one fewer lumbar vertebra (7C, 13T, 3L; Williams et al., 2019a). The  
64 latter presacral combination is frequently found in western gorillas, chimpanzees, and bonobos as well  
65 (Williams et al., 2019a). Orangutans generally have one fewer thoracic vertebra than chimpanzees,  
66 bonobos, and western gorillas (7C, 12T, 4L). Hylobatids (lesser apes or gibbons) are highly variable but  
67 most commonly possess 7C, 13T, and 5L. Modern humans are also variable in their vertebral formula,  
68 although deviations from the modal formula are less frequent than in most other apes. Humans normally  
69 have 7C, 12T, and 5L (Pilbeam, 2004; Williams et al., 2019a).

70         A variety of approaches have been brought to bear on this question, including parsimony  
71 analyses, comparative morphology, and inferences from fossil taxa (Pilbeam, 2004; McCollum et al.,  
72 2010; Williams, 2012a; Williams et al., 2019a; Machnicki and Reno, 2020). Two formal ancestral state  
73 reconstruction studies have been performed so far (Fulwood and O’Meara, 2014; Thompson and  
74 Almécija, 2017). Both studies found strongest support for the short back model and weakest support for  
75 the long back model. Fulwood and O’Meara (2014), however, looked only at lumbar numbers.

76 Thompson and Almécija (2017) examined all precaudal vertebrae, but each portion of the vertebral  
77 column was analyzed independently. This represents a major limitation of their study (which they  
78 acknowledge), since conducting the analysis in this way assumes that all changes to different segments  
79 of the vertebral column are independent of one another.

80 Although vertebral formulae (regional numbers of vertebrae) can clearly evolve via meristic  
81 change (additions or deletions of vertebrae), which is largely independent in each region of the vertebral  
82 column, homeotic changes (regional boundary shifts within the same numerical framework) also appear  
83 to be common both inter- and intraspecifically (Galis, 1999b; Wellik and Capecchi, 2003; Williams,  
84 2011; Galis et al., 2014; Williams and Pilbeam, 2021). For example, cercopithecoid monkeys tend to  
85 possess either 13T and 6L or 12T and 7L (Schultz and Straus, 1945; Clausier, 1980; Williams, 2011,  
86 2012a), two configurations of 19 thoracic and lumbar vertebrae achievable via homeotic shifts at the  
87 thoracolumbar border. Most researchers agree that great apes evolved reduced numbers of lumbar  
88 vertebrae via homeotic shifts at the lumbosacral border and that hominoid sacra increased in number due  
89 to homeotic shifts at the lumbosacral border or the sacrocaudal border (see Williams and Russo, 2015).  
90 Recently, Williams and Pilbeam (2021) proposed that hominins evolved from a  $LCA_{H-P}$  that was  
91 specifically panin-like in its full vertebral formula and derived the modal human configuration via a  
92 single homeotic shift in Hox10 rostral and caudal expression boundaries.

93 Homeobox (Hox) gene expression domains are associated with vertebra regional boundaries and  
94 are thought to contribute to the development of morphologies typical of different regions (Wellik and  
95 Capecchi, 2003; Carapuço et al., 2005; Mallo et al., 2010; Casaca et al., 2014). Shifts in Hox gene  
96 expression domains and their effects on vertebra development are therefore homeotic in nature. Since  
97 differences among taxa in regional numbers of vertebrae can result from meristic or homeotic change at  
98 any regional boundary, ideally full vertebral formulae (cervical, thoracic, lumbar, sacral,  
99 caudal/coccygeal) should be used in analyses, rather than considering each individual section  
100 independently. Here, we employ phylogenetic ancestral state reconstruction methods that account for

101 both homeotic and meristic changes on full vertebral formulae of primates to understand how vertebral  
102 numbers evolved and test hypotheses regarding the number of vertebrae in ancestral apes.

103

## 104 **2. Materials and methods**

### 105 *2.1. Samples*

106 Data were collected at natural history museums and university collections around the world  
107 (Supplementary Online Material [SOM] Table S1). Specimens were articulated to check for  
108 completeness, and numbers of cervical, thoracic, lumbar, and caudal (or coccygeal in the case of animals  
109 lacking an external tail) vertebrae were recorded. The number of elements composing the sacrum and the  
110 number of coccygeal segments (if relevant) were recorded. Taxa were included in the analysis if they  
111 were represented by at least four individuals in the dataset. The Schultz (1961) definition of thoracic and  
112 lumbar vertebrae based on rib presence (thoracic) or absence (lumbar) was used (also see Schultz and  
113 Straus, 1945; Williams and Pilbeam, 2021). For the purposes of this study, individuals with incomplete  
114 homeotic transitions (e.g., 12.5 thoracic and 4.5 lumbar) were treated as half a count for each whole  
115 number vertebral formula (e.g., 0.5 for 13 thoracic / 4 lumbar and 0.5 for 12 thoracic / 5 lumbar) rather  
116 than individuals with unique formulae. The total sample includes 6216 individuals representing 141  
117 species (Table 1).

118

### 119 *2.2. Phylogeny*

120 For this analysis, we used the recent mammal phylogeny published by Upham and colleagues (2019).  
121 This phylogeny strongly samples both primate and non-primate taxa and is better resolved than earlier  
122 mammal phylogenies (e.g., Bininda-Emonds et al., 2007). We could not use an order-wide primate  
123 phylogeny as those in common use (e.g., Arnold et al., 2010; Springer et al., 2012) do not include  
124 sufficient outgroups for the primate-wide analysis.

125

126 2.3. *Data analysis*

127 We performed two ancestral character state reconstructions. Due to computational limitations, we  
128 were unable to include variation in all types of vertebrae across all primates. Therefore, we limited our  
129 analysis of the entire primate order (and relevant outgroups) to precaudal vertebrae. For our analysis that  
130 included caudal vertebrae we focused on apes specifically, which allowed us to use fewer taxa and  
131 character states, and thus make the analysis computationally feasible.

132 We performed ancestral state reconstructions using the `make.simmap` and `describe.simmap`  
133 functions in the `phytools` package (Revell, 2012) in the R statistical environment using R v. 4.1.1 (R  
134 Core Team, 2022). The `make.simmap` function implements the stochastic character mapping method of  
135 Bollback (2006), and `describe.simmap` summarizes the posterior distributions of all simulations.  
136 SIMMAP simulates character state transition across the tree under an instantaneous transition rate, or  
137  $M_k$  model (Lewis, 2001). Rates of transitions between different character states are represented using an  
138 instantaneous rate matrix (Q matrix). The SIMMAP method can accommodate uncertainties in tip states.  
139 These simulations can be run multiple times, and a posterior distribution of states is generated for each  
140 node and tip. For each reconstruction, we generated 5000 character histories. Posterior probabilities for  
141 ancestral states at each node represent the frequency that each state appears at that node across those  
142 5000 stochastic simulations. Once the simulations were run, we examined both the posterior probability  
143 of different character states at relevant nodes in the primate tree as well as the 95% highest posterior  
144 density (HPD) intervals for each vertebral type at each node. The HPD interval represents the range of  
145 values that includes 95% of the posterior distribution, centered on the value with the highest posterior  
146 probability. HPD intervals were calculated using the `HPDintervals` function in the `coda` package in R  
147 (Plummer et al., 2006).

148 In the first reconstruction (Analysis 1), we examined the precaudal vertebral numbers across  
149 Primates. To allow us to estimate ancestral conditions near the base of the primate tree, we also included  
150 data from the four orders most closely related to Primates: Dermoptera, Scandentia, Lagomorpha, and

151 Rodentia. Outgroup taxa were chosen to be representative of the diversity of different vertebral formulae  
152 in these groups. Dermoptera is represented by two extant genera, Scandentia is represented by six  
153 species representing both extant families, Lagomorpha is represented by a single species (*Lepus*  
154 *timidus*), and Rodentia is represented by nine species from nine families (see Table 1). Ideally, our  
155 sample would have included pikas within Lagomorpha. We encountered very few specimens during data  
156 collection, however, and Tague's (2017) large samples of lagomorphs cannot be compiled with our data  
157 due to differences in data collection (i.e., Tague, 2017 did not follow the Schultz criteria in recording  
158 'half counts' for asymmetrical, 'intermediate' vertebrae).

159         Possible character states for each section of the column include: cervical (7), thoracic (12 or  
160 fewer, 13, 14, 15 or more), lumbar (3, 4, 5, 6, 7, 8 or more), and sacral (2, 3, 4, 5, 6, 7). Together, these  
161 make 144 unique character states. Prior probabilities were applied to each tip based on the frequency  
162 that a given condition is observed in a given taxon in our dataset. All absolute frequencies over 10%  
163 were included. In addition, we ran a broken stick model (MacArthur, 1957) to determine whether any  
164 variants represented at below 10% frequency should also be included. Variants were included if they  
165 were represented in more than 10% of individuals or were represented in fewer than 10% of individuals  
166 but in more individuals than would be expected under a random distribution. None of the character states  
167 eliminated during binning (e.g., 11 thoracic vertebrae binned with 12) represented a majority or plurality  
168 of any taxon studied.

169         The Q matrix (the instantaneous rate matrix for the  $M_k$  model) is calculated using maximum  
170 likelihood, contingent on tip states, and a specified rate heterogeneity. The default rate heterogeneity in  
171 the `make.simmap` function is a symmetrical model in which transitions between each pair of character  
172 states occur at the same rate in both directions, but transitions between different pairs occur at different  
173 rates. For example, the rate of a transition between 7C-12T-7L-3S  $\rightarrow$  7C-13T-6L-3S is the same as 7C-  
174 13T-6L-3S  $\rightarrow$  7C-12T-7L-3S, but 7C-12T-7L-3S  $\leftrightarrow$  7C-12T-7L-4S is different. Using this default model  
175 in our analyses, however, would involve 10,000 unique rate parameters, which is unfeasible. An



176 alternative model is an equal rates model, in which transitions among all character states occur at the  
177 same rate. This model involves only a single rate parameter, but it means, for example, that a change  
178 between 7C-12T-7L-3S ↔ 7C-13T-6L-3S (a single homeotic shift) occurs at the same rate as a change  
179 from 7C-12T-7L-3S ↔ 7C-14T-3L-6S (multiple homeotic and meristic shifts), which is incompatible  
180 with current research on vertebral development.

181 In light of these issues with the default models, we used a custom model that accounts for prior  
182 understanding of how numbers of vertebrae evolve while also minimizing the number of parameters in  
183 the model. Our model (SOM Table S2) included only two types of character transitions: the addition or  
184 removal of one vertebra (representing a meristic change); and a vertebra changing from one type into a  
185 neighboring type (representing a homeotic change). The rates of homeotic and meristic changes are  
186 independent of one another, but the model assumes that all homeotic transitions happen at the same rate,  
187 and all meristic transitions happen at the same rate. All other types of transitions were set to a rate of 0.  
188 This means that it is not possible for a lineage to gain or lose two vertebrae at the same time, but since  
189 the  $M_k$  model treats transitions as instantaneous, independent, and reversible, it is possible for two  
190 transitions to occur along the same branch of the tree, leading to multiple changes between adjacent  
191 nodes (made more likely the longer the branch is).

192 In the second reconstruction (Analysis 2), we examined the full vertebral column numbers,  
193 including caudal/coccygeal vertebrae, in apes. As outgroups for apes, we included a representative  
194 sampling of cercopithecoids and platyrrhines, as well as a tarsier. By limiting the analysis in this way we  
195 could use fewer taxa and possible character states and therefore make the analysis that included caudal  
196 vertebrae computationally feasible. Possible character states for each section of the column include:  
197 Cervical (7); Thoracic (12, 13, 14 or more); Lumbar (3, 4, 5, 6, 7 or more); Sacral (3, 4, 5, 6); Caudal (2,  
198 3, 4, 5, 6 or more). Together, these make a total of 300 character states. To reduce this number and  
199 improve computation time, we first ran 100 simulations and examined which areas of morphospace were  
200 utilized in those simulations. We found that no lineage in any of these 100 simulations ever passed

201 through a condition of having 12 thoracic vertebrae and 3 lumbar vertebrae or 14 thoracic vertebrae and  
202 7 lumbar vertebrae. We therefore eliminated these possibilities to improve computation time, leaving  
203 260 possible character states. As with the first analysis, prior probabilities were applied to each tip based  
204 on the frequency that a given condition is observed in a given taxon in our dataset. All absolute  
205 frequencies over 10% were included, and a broken stick model was used to determine whether  
206 additional variants with absolute frequencies below 10% should be included. Several hylobatid species  
207 lacked four individuals with caudal counts. These taxa were included using a uniform prior for each  
208 possible caudal length except 6+ (presence of an external tail). Except for variation in tail length, which  
209 is condensed into the single state of 6+ caudal vertebrae (i.e., possessing a tail), none of the character  
210 states eliminated during binning (e.g., 15 thoracic vertebrae binned with 14) represented a majority or  
211 plurality of any taxon studied.

212 As with Analysis 1, practical and theoretical concerns precluded the use of default models for the  
213 rate heterogeneity of the Q matrix and we therefore used a custom model (SOM Table S3). In Analysis  
214 2, we set three unique rates for the Q matrix: the addition or removal of one vertebra (representing a  
215 meristic change); a vertebra changing from one type into a neighboring type (representing a homeotic  
216 change); and any changes between 5 and 6+ caudal vertebrae. Because of the large amount of variation  
217 binned in the 6+ state, it would be inappropriate to treat a transition from 5 to 6+ caudal vertebrae as  
218 identical to a transition from 5 to 4 caudal vertebrae. As in Analysis 1, other types of transitions were set  
219 to a rate of 0.

220

### 221 **3. Results**

222

#### 223 *3.1. Analysis 1*

224 Posterior probabilities for all vertebral formulae in Analysis 1 are given in SOM Table S4, and  
225 95% HPD are given in SOM Table S5. A high-level summary of results is given in Table 2. Additional

226 summaries of results showing only different thoracic (SOM Table S6; SOM Fig. S1), lumbar (SOM  
227 Table S7; SOM Fig. S2), sacral (SOM Table S8; SOM Fig. S3), precaudal (SOM Table S9; SOM Fig.  
228 S4), and presacral (SOM Table S10; SOM Fig. S5) counts are given in the SOM. Node labels used in  
229 SOM Tables S4–S10 are shown in the tree in SOM Figure S6.

230 Analysis 1 shows that vertebral numbers are fairly conserved in primates, especially within  
231 major primate clades: Anthroidea, Platyrrhini, and Catarrhini are all reconstructed, with strong  
232 support, as having 29 precaudal vertebrae (>95% posterior probability for all three clades, 95% HPD  
233 includes only 29 presacral vertebrae) and 26 presacral vertebrae (>88% for all three clades, 95% HPD is  
234 26–25 for anthropoids and catarrhines and 26 only for platyrrhines). The single formula with the highest  
235 posterior probability is 7C-13T-6L-3S (anthropoids 80%; catarrhines 69%; platyrrhines 95%). Twenty-  
236 six presacral vertebrae is also the condition recovered for the last common ancestor of haplorhines (87%;  
237 95% HPD 26–27) and primates as a whole (86% 95% HPD 26–27). Twenty-nine precaudal vertebrae is  
238 also most common at these nodes but support is more tentative (65% for haplorhines, 95% HPD 29–30;  
239 54% for primates, 95% HPD 29–31), with 30 precaudal vertebrae being the most probable alternative  
240 (35% for haplorhines, 45% for primates). Ancestral primates probably had 13 thoracic vertebrae (79%;  
241 12 thoracic vertebrae 20%; 95% HPD 12–13), six lumbar vertebrae (67%; 95% HPD six to seven), and  
242 three sacral vertebrae (67%; 95% HPD three to four). In haplorhines, the specific formulae with the  
243 highest posterior probabilities are 7C-13T-6L-3S (48%), 7C-13T-6L-4S (22%), and 7C-12T-7L-3S  
244 (15%). In primates, the most commonly recovered ancestral condition is 7C-13T-6L-3S (38%), although  
245 7C-13T-6L-4S (28%) and 7C-12T-7L-3S (15%) are also common. An overview of primate vertebral  
246 evolution, showing the formulae with the highest posterior probabilities, is given in Figure 2.

247 Nearly all haplorhine subgroups down to the family level (except Aotidae) retain the ancestral  
248 haplorhine condition of 29 precaudal vertebrae (Platyrrhini, Pitheciidae, Callitrichidae, Catarrhini,  
249 Cercopitheciidae, Hominoidea, Hylobatidae, Tarsiidae all >95% posterior probability and 95% HPD 29  
250 only; Atelidae 92% posterior probability, 95% HPD 28–29; Hominidae 95% HPD 28–29; Cebidae 74%

251 posterior probability, 95% HPD 29–30). The ancestral haplorhine condition of 26 presacral vertebrae is  
252 also retained in the ancestors of most major haplorhine clades (Platyrrhini, Pitheciidae, Callitrichidae,  
253 Cercopithecidae, Tarsiidae all >95%, 95% HPD 26 only; Atelidae 92%, 95% HPD 25–26; Cebidae 74%,  
254 95% HPD 26–27; Catarrhini 88% 95% HPD 25–26). We recovered strong support for an ancestral  
255 condition of 7C-13T-6L-3S for platyrrhines (95%) and one of its families, Pitheciidae (93%), and more  
256 tentative support among other platyrrhine families (Callitrichidae: 66%, Cebidae: 72%). We also found  
257 tentative support for this formula being the ancestral condition of all catarrhines (68%). We recovered  
258 strong evidence for homeotic shifts in thoracic and lumbar counts at the base of families Cercopithecidae  
259 and Atelidae. Cercopithecids evolved a longer lower back with extremely strong support for an ancestral  
260 condition of 7C-12T-7L-3S (99%). Atelids evolved a shorter lumbar column; the most commonly  
261 recovered condition was 7C-14T-5L-3S (89%).

262 We recovered strong support for a reduced presacral count of 25 presacral vertebrae in ancestors  
263 of both hominoids (93%, 95% HPD 24–25) and atelines (96%; 95% HPD includes only 25). Twenty-five  
264 presacral vertebrae was retained in hylobatids (>99%), but a further reduction in the presacral count to  
265 24 was recovered for hominoids (91%; 95% HPD 23–24). The single formula for the ancestor of atelines  
266 with the highest posterior probability is 7C-14T-4L-3S (95%). In atelines, reduction to four lumbar  
267 vertebrae was accomplished by a meristic change as there is no concomitant increase in sacral numbers,  
268 in contrast with hominoids. In hominoids and hominids, the reduction in presacral vertebrae was  
269 accomplished through homeotic transitions, and there is a concomitant reduction in lumbar vertebrae  
270 and increase in the number of sacral vertebrae. The most common single formula recovered as ancestral  
271 for hominoids is 7C-13T-5L-4S (89%) and the most common single formula recovered as ancestral for  
272 hominids is 7C-13T-4L-5S (86%).

273 We recovered evidence for several additional shifts within Hominidae. *Pongo* underwent a  
274 meristic shift, losing a single thoracic vertebra to 7C-12T-4L-5S (94%). The last common ancestor of  
275 Homininae retained the ancestral hominid formula of 7C-13T-4L-5S (70%; the next most common is

276 7C-13T-4L-6S, at 18%). The last common ancestor of chimpanzees and humans also likely retained this  
277 vertebral formula (59%), although an increase in the number of sacral vertebrae to 7C-13T-4L-6S also  
278 receives some support (35%). The last common ancestor of both species of *Pan* either evolved or  
279 retained this latter formula (77%). *Gorilla* underwent a homeotic shift reducing the number of lumbar  
280 vertebrae and increasing the number of sacral vertebrae to 7C-13T-3L-6S (86%). An overview of  
281 hominid vertebral evolution, showing the formulae with the highest posterior probabilities, is given in  
282 Figure 3.

283 The ancestral strepsirrhine is tentatively recovered as having 30 precaudal vertebrae (68%  
284 posterior probability), an increase in one from the ancestral primate, although 29 precaudal vertebrae  
285 (22%) also represents a substantial minority (95% HPD 29–31). The number of presacral vertebrae in  
286 the ancestral strepsirrhine is recovered as being either 26 (43%) or 27 (54%) (95% HPD 26–27). The  
287 most probable single formula is 7C-13T-7L-3S (39%). The only other formulae above 10% posterior  
288 probability are the possible ancestral primate formulae, 7C-13T-6L-4S (16%) and 7C-13T-6L-3S (13%).  
289 This pattern was retained in ancestral lemuroids (30 precaudal: 71%; 29 precaudal 26%; 95% HPD 29-  
290 30; 27 presacral: 61%; 26 presacral: 37%; 95% HPD 26–27; most common single formula: 7C-13T-7L-  
291 3S, 45%; 7C-12T-7L-3S, 7C-12T-8L-3S, and 7C-13T-6L-3S are all between 11 and 14%). Indriids  
292 further increase the number of lumbar vertebrae to eight through a homeotic transition at the  
293 thoracolumbar border, with the most common formula being 7C-12T-8L-3S (99%).

294 We recovered substantial changes at the base of Lorisiformes. Lorisiformes are found to evolve  
295 an additional sacral (four sacral, 70%; five sacral, 17%; 95% HPD three to five) and at least one  
296 additional presacral vertebra (28 presacral: 56%), possibly two (29 presacral: 26%; 95% HPD 27-29).  
297 These additional presacral vertebrae were likely thoracic vertebrae (14 thoracic: 60%; 15 thoracic: 32%;  
298 95% HPD 13–15 thoracic), and the most common ancestral lorisoid formulae are 7C-14T-7L-4S (35%)  
299 and 7C-15T-7L-4S (17%). No others are above 8%. Galagids are found to have reduced the number of  
300 vertebrae, with 13 thoracic vertebrae (82%; 95% HPD 13–14), 6 lumbar vertebrae (96%), and 3 sacral

301 vertebrae (97%). The most common single formula is the most probable ancestral primate formula, 7C-  
302 13T-6L-3S (76%; 7C-14T-6L-3S has the next highest posterior probability at 16%).

303

### 304 3.2. *Analysis 2*

305 Posterior probabilities for all vertebral formulae in Analysis 2 are given in SOM Table S11, and  
306 95% HPD are given in SOM Table S12. A high-level summary of results is given in Table 3. Additional  
307 summaries of results showing only different thoracic (SOM Table S13; SOM Fig. S7), lumbar (SOM  
308 Table S14; SOM Fig. S8), sacral (SOM Table S15; SOM Fig. S9), caudal/coccygeal (SOM Table S16;  
309 SOM Fig. S10), precaudal (SOM Table S17; SOM Fig. S11), and presacral (SOM Table S18; SOM Fig.  
310 S12) counts are given in the SOM. Node labels used in SOM Tables S11–S18 are shown in the tree in  
311 SOM Figure S13.

312 In Analysis 2, with its more limited taxonomic scope, the resolution of clades above the  
313 superfamily level is poor. The ancestral catarrhine pattern with the highest posterior probability is 26  
314 presacral vertebrae (57%), 29 precaudal vertebrae (67%), and an external tail (94%). Twenty-five  
315 presacral (38%) and 28 precaudal (27%) also have notable posterior probabilities. Ninety-five percent  
316 HPD is 25–26 presacral and 27–29 precaudal. The most probable single formulae are 7C-13T-6L-3S-  
317 6+Ca (27%) and 7C-12T-7L-3S-6+Ca (23%).

318 The common ancestor of hominoids likely underwent a shift to a lower presacral count (25  
319 presacral vertebrae: 69%; 24 presacral vertebrae: 27%; 95% HPD 24–25). The precise vertebral formula  
320 at the base of Hominoidea is poorly resolved, but this reduction in presacral vertebrae is very likely  
321 driven by a reduced number of lumbar vertebrae (five lumbar vertebrae: 69%; four lumbar vertebrae:  
322 19%; 95% HPD four to six). The most common formula is 7C-13T-5L-4S-3Ca (19%), and only four  
323 individual formulae are above 5% posterior probability (7C-13T-5L-4S-4Ca: 17%; 7C-13T-5L-5S-3Ca:  
324 14%; 7C-13T-4L-5S-3Ca: 7%). The ancestral hominoid likely had either three (58%) or four (36%)  
325 coccygeal vertebrae (95% HPD two to four).

326 The last common ancestor of hylobatids is firmly resolved as having had 25 presacral vertebrae,  
327 including five lumbar vertebrae (>99% for both). The most common single formula is 7C-13T-5L-4S-  
328 3Ca (67%). The last common ancestor of hominids is recovered as having 24 presacral vertebrae (75%;  
329 95% HPD 23-25), including four lumbar vertebrae (76%; 95% HPD four to five). The number of  
330 precaudal and total vertebrae in the last common ancestor of hominids is more poorly resolved (32 total  
331 vertebrae: 47%; 33 total vertebrae: 43%; 29 precaudal: 60%; 30 precaudal: 30%; 95% HPD 28–30), in  
332 part due to uncertainty over the number of sacral vertebrae the ancestral hominid had (five [57%] or six  
333 [37%] are the most common; 95% HPD four to six). The ancestral hominid is resolved as having three  
334 caudal vertebrae (75%; 95% HPD two to four). The most common precise formulae for the last common  
335 ancestor of hominids are 7C-13T-4L-5S-3Ca (27%), 7C-13T-4L-6S-3Ca (20%), and 7C-13T-4L-5S-4Ca  
336 (10%).

337 Ancestral hominines are recovered as having 24 presacral vertebrae (83%; 95% HPD 23–24),  
338 including four lumbar vertebrae (85%; 95% HPD three to five), likely six (67%) or possibly five (33%)  
339 sacral vertebrae (95% HPD five to six), and three (72%; 95% HPD two to four) caudal vertebrae. The  
340 most common single formula is 7C-13T-4L-6S-3C (39%). This ancestral hominine pattern is retained in  
341 the last common ancestor of chimpanzees and humans, with 24 presacral vertebrae (93%; 95% HPD 23  
342 or 24), four lumbar vertebrae (89%; 95% HPD four or five), six sacral vertebrae (70%; 95% HPD five or  
343 six) and three caudal vertebrae (63%; 95% HPD two to four). The most common single formula is 7C-  
344 13T-4L-6S-3Ca (43%). No other formulae are above 15%, although 7C-13T-4L-5S-4Ca has 14%, and  
345 formulae that are +/- one caudal vertebrae total 59%. Formulae that involve 33 total vertebrae were  
346 reconstructed in 64% of simulations. *Gorilla* may have undergone a reduction in the number of both  
347 lumbar (three lumbar vertebrae: 63%; four lumbar vertebrae 37%; 95% HPD three to four) and caudal  
348 (two caudal vertebrae: 46%; three caudal vertebrae; 46%; 95% HPD two to four) vertebrae. The most  
349 common formulae for the ancestor of *Gorilla* are 7C-13T-3L-6S-2Ca (39%) and 7C-13T-4L-6S-3Ca  
350 (30%). *Pongo* underwent a reduction in presacral vertebrae (23 presacral vertebrae: >99%) due to a

351 meristic loss of a thoracic vertebra (12 thoracic vertebrae: >99%). The most common formula for the  
352 ancestor of crown *Pongo* is 7C-12T-4L-5S-3Ca (63%), with 7C-12T-4L-6S-3Ca (24%) notable as well.

353

#### 354 **4. Discussion**

355 We performed two ancestral state reconstructions, Analysis 1, which includes a broad sampling  
356 of primates and euarchontaglirans, but excludes caudal vertebrae counts, and Analysis 2, which focuses  
357 on hominoids and appropriate outgroups, and includes caudal vertebral counts. Results of Analyses 1  
358 and 2 are broadly similar, but Analysis 1 has greater resolution at most nodes. The additional uncertainty  
359 in Analysis 2 compared with Analysis 1 makes sense since Analysis 2 includes fewer taxa and more  
360 potential variants (inclusion of caudal/coccygeal vertebra number). Despite this, the results of both  
361 analyses generally look similar in how they relate to the long back, intermediate back and short back  
362 models: Hominoids are found to depart from most other primates (and mammals; Williams et al., 2019b)  
363 in reducing their number of presacral vertebrae from 26 to 25, and hominids reduce this further from 25  
364 to 24. The biggest difference between the two analyses is in the number of sacral vertebrae in hominines  
365 and the  $LCA_{H.P.}$ . Analysis 1 recovers somewhat stronger support for 5 sacral vertebrae, whereas Analysis  
366 2 recovers more substantial support for 6 sacral vertebrae at both nodes. Interestingly, the previous  
367 ancestral state reconstruction on vertebral formulae also reported quite a bit of uncertainty regarding the  
368 presence of five or six sacral vertebrae at this node, despite utilizing somewhat different methods and  
369 incorporating fossil taxa (Thompson and Alméjida, 2017). Given that chimpanzees, bonobos, and  
370 western gorillas are all highly polymorphic for these traits, this uncertainty is perhaps unsurprising and  
371 may represent real variation in ancestral hominoids.

372 Overall, our results strongly support the hypothesis that lumbar reduction is a shared derived trait  
373 of hominoids (Pilbeam, 2004; Williams, 2012a; Williams and Russo, 2015; Williams and Pilbeam, 2021)  
374 and reject the hypothesis that hominoids retained a long lower back throughout much of their evolution  
375 (Lovejoy et al., 2009; Lovejoy and McCollum, 2010; McCollum et al., 2010; Machnicki and Reno,



376 2020). The reduction of lumbar vertebrae to five or fewer early in ape evolution is strongly supported,  
377 while the retention of six lumbar vertebrae in ancestral apes receives much weaker support (Tables 2 and  
378 3). Support for lumbar reduction to four or fewer in great apes is also strong, while the retention of six  
379 lumbar vertebrae in ancestral great apes or the  $LCA_{H-P}$  receives effectively no support. Indeed, in  
380 Analysis 1, six or more lumbar vertebrae were never recovered at either of these nodes in any of the  
381 5000 simulations we ran (SOM Table S4) and the support was not much better in Analysis 2 (SOM  
382 Table S11).

383         The observed reduction of presacral vertebrae at the base of both hominoids and hominids was  
384 accomplished through homeotic shifts at the lumbosacral border, and numbers of precaudal vertebrae  
385 remain largely consistent (Fig. 3). These results are consistent with the hypothesis that rostral shifts in  
386 the Hox11 expression domain may be responsible for these changes (Davis and Capecchi, 1994; Favier  
387 et al., 1995; Wahba et al., 2001; Wellik and Capecchi, 2003; McIntyre et al., 2007). This mechanism for  
388 shortening the lumbar column is different than that observed in atelids. In atelids, convergent lumbar  
389 shortening was accomplished via caudal shift at the thoracolumbar border, and in the case of atelines,  
390 meristic loss of a presacral element (Fig. 2).

391         The most probable scheme we recover for the evolution of the vertebral column in apes (Fig. 3)  
392 is that ancestral catarrhines had the formula 7C-13T-6L-3S with a tail, or were perhaps polymorphic for  
393 7C-13T-6L-3S and 7C-12T-7L-3S. Tail loss (reduction and change in morphology from caudal to  
394 coccygeal vertebrae; Russo, 2015) probably characterized the ancestor of crown hominoids, a condition  
395 likely inherited from stem hominoids such as *Ekembo* and *Nacholapithecus* (Ward et al., 1991;  
396 Nakatsukasa et al., 2003, 2004; Russo, 2016). We recover three or four coccygeal vertebrae as the most  
397 likely counts for the ancestor of extant apes. In our analysis, ancestral crown apes exhibited a homeotic  
398 shift at the lumbar-sacral border to 7C-13T-5L-4S (Fig. 3). This precaudal pattern was retained in  
399 ancestral hylobatids. The lumbar reduction we observe in crown apes is consistent with the previous  
400 formal ancestral state reconstruction on this topic (Thompson and Alméjija, 2017). That study did report

401 the strongest support for 12 thoracic vertebrae in ancestral apes, but the authors expressed very little  
402 confidence in this result. They considered 12 thoracic vertebrae a likely consequence of limited  
403 outgroups and fossil taxa that were dominated by cercopithecoids and hominins, respectively, a  
404 conclusion that is consistent with our study, and its larger outgroup sample, reconstructing 13 thoracic  
405 vertebrae at this node.

406         In our study, we find that ancestral great apes further reduced their presacral vertebrae through an  
407 additional homeotic shift at the lumbosacral border, changing their formula to 7C-13T-4L-5S.  
408 Orangutans reduced their thoracic count through a meristic shift to 7C-12T-4L-5S, and gorillas further  
409 reduced their lumbar count through another homeotic shift at the lumbosacral border to 7C-13T-3L-6S.  
410 This result contrasts with previous studies that argue for a crown *Gorilla* node with four lumbar  
411 vertebrae (Pilbeam, 2004; Williams, 2011, 2012a; Williams and Russo, 2015; Williams et al., 2016,  
412 2019b; Williams and Pilbeam, 2021). However, the other published formal ancestral state reconstruction  
413 (Thompson and Alméjida, 2017) found the same result reported here at the gorilla node. We attribute this  
414 discrepancy to the high incidence of three lumbar vertebrae in eastern gorillas (*G. beringei*) and the  
415 highly polymorphic presence of three and four lumbar vertebrae in western gorillas (*G. gorilla*). Still,  
416 our results point to a great deal of uncertainty at the ancestral *Gorilla* node. One possible interpretation  
417 of these results is that the last common ancestor of gorillas was polymorphic for three and four lumbar  
418 vertebrae, as are modern western gorillas, but a founder effect led to the loss of the four lumbar character  
419 state in eastern gorillas (Williams, 2012a). Since ancestral state reconstruction methods (including both  
420 the one used here and the one used by Thompson and Alméjida [2017]), typically model polymorphism  
421 as uncertainty surrounding a hypothetical ‘true’ character state, such a scenario would be modeled as  
422 exactly the result observed here—with high uncertainty at both the root node and one daughter node, and  
423 the second daughter node with high certainty. Unfortunately, it is not possible to differentiate such a  
424 scenario from actual uncertainty.

425

426 4.1. *The last common ancestor of Homo and Pan*

427 LCA<sub>H-P</sub>, likely either retained the ancestral hominid formula of 7C-13T-4L-5S or possessed a  
428 longer sacrum (7C-13T-4L-6S). The latter count suggests that the LCA<sub>H-P</sub> may have had an additional  
429 precaudal vertebra, making it more similar to bonobos than to chimpanzees (McCollum et al., 2010).  
430 Given that most extant African apes, particularly chimpanzees, bonobos, and western gorillas, are highly  
431 polymorphic for vertebral counts, it is possible that ancestral apes were as well (Pilbeam, 2004;  
432 McCollum et al., 2010; Williams et al., 2016). This polymorphism may be due to a relaxation of  
433 selection pressures for mobility at the lumbosacral margin (Galis et al., 2014; Shapiro and Kemp, 2019;  
434 Williams et al., 2019b), and possibly related to stiffening of the lower back through lumbar entrapment  
435 (Lovejoy and McCollum, 2010; McCollum et al., 2010; Machnicki et al., 2016b; Williams et al., 2019a).  
436 A polymorphic condition of five or six sacral vertebrae in the LCA<sub>H-P</sub> seems likely and would be  
437 consistent with our results. This scenario is also consistent with published short back scenarios (Pilbeam,  
438 2004; Williams, 2012a; Williams and Russo, 2015; Williams et al., 2016, 2019a; Williams and Pilbeam,  
439 2021), but contradicts long-back (Lovejoy et al., 2009; Lovejoy and McCollum, 2010; McCollum et al.,  
440 2010, 2010; Machnicki and Reno, 2020) and intermediate back (Latimer and Ward, 1993; Haeusler et  
441 al., 2002; Machnicki et al., 2016; Tardieu and Haeusler, 2019) models.

442 Of the three scenarios that have been proposed to explain the condition from which hominins  
443 evolved, neither the intermediate back model nor the long back model is supported by this study,  
444 although counts consistent with the intermediate back model fall within the 95% HPD LCA<sub>H-P</sub> node in  
445 Analysis 2 and thus cannot be fully rejected here. We counted the minimum number of changes in  
446 vertebral numbers (via either homeotic or meristic change) at major nodes (i.e., hominoid, hylobatid,  
447 hominid, hominine, hominin, and the ancestral *Pongo*, *Gorilla*, and *Pan* nodes) in each model (note that  
448 in the long back model, proposed parallel changes in *Pan paniscus* and *Pan troglodytes* are not counted  
449 here). The long back models (McCollum et al., 2010; Machnicki et al., 2016a; Machnicki and Reno,  
450 2020) require 11–15 or more changes (minima of 11 in McCollum et al., 2010; 15 in Machnicki et al.,

451 2016; 13 in Machnicki and Reno, 2020; see their figures 4, 2, and 6, respectively) and the predicted  
452 vertebral formulae fall outside of the 95% HPD range in our study and receive 0% or near 0% posterior  
453 probabilities. The intermediate back models (Latimer and Ward, 1993; Haeusler et al., 2002) require  
454 eight or more changes (see figure 9 in Haeusler et al., 2002 and figure 3 in Machnicki et al., 2016) and  
455 fare only slightly better in terms of posterior probabilities in our study. The condition of having five  
456 lumbar vertebrae, as predicted by the intermediate back model, does fall within the 95% HPD range for  
457 the hominoid and hominid nodes in both analyses, as well as the hominine and  $LCA_{H-P}$  node in Analysis  
458 2, however, so we are unable to fully reject it here.

459         There are several versions of the short back model (Pilbeam, 2004; Williams, 2012a; Williams et  
460 al., 2016, 2019a; Williams and Pilbeam, 2021), which receive the highest posterior probabilities by far in  
461 our analysis. Most short back models, which propose the presence of 13 thoracic vertebrae and gains to  
462 the number of sacral vertebrae via lumbar sacralization (i.e., homeotic shifts at the lumbosacral border;  
463 Pilbeam, 2004; Williams, 2011, 2012; Williams and Russo, 2015; Williams et al., 2016, 2019a; Williams  
464 and Pilbeam, 2021) require five changes. Regarding the  $LCA_{H-P}$ , all short back models propose either  
465 7C-13T-4L-5S (Williams, 2011, 2012a; Williams and Russo, 2015; Williams et al., 2016) or 7C-13T-4L-  
466 6S (Pilbeam, 2004; Williams and Pilbeam, 2021). These receive the highest and second highest support  
467 in both of our analyses. Analysis 1 recovers the best support for 7C-13T-4L-5S, while Analysis 2  
468 recovers strongest support for 7C-13T-4L-6S. In Analysis 2, we found the strongest support for a  $LCA_{H-P}$   
469 condition of 7C-13T-4L-6S-3Ca. The second most strongly supported condition was 7C-13T-4L-5S-4Ca,  
470 which represents a homeotic variant of the variant with the strongest support. Indeed, we found  
471 moderately strong support for a  $LCA_{H-P}$  with 33 total vertebrae. A modal number of 33 total vertebrae is  
472 found in humans, chimpanzees, bonobos, and western gorillas. Although high amounts of variation are  
473 seen in specific vertebral numbers within each species, when vertebrae are grouped into combined  
474 presacral (C+T+L) and sacrocaudal (S+Ca) numbers, there is much less (i.e., there is a great deal of

475 variation in specific vertebral formula, but most individuals have 24 presacral vertebrae and 9  
476 sacrococcygeal vertebrae; Williams & Pilbeam, 2021)

477

#### 478 4.2. *Ancestral Primates*

479 Primates are tentatively reconstructed with 26 presacral and 3 sacral vertebrae, similar to many  
480 mammals (Pilbeam, 2004; Narita and Kuratani, 2005; Williams, 2011; Galis et al., 2014; Williams et al.,  
481 2019b). There is a large amount of uncertainty regarding specific formulae, however. The formula with  
482 the highest posterior probability is 7C-13T-6L-3S, although 7C-13T-6L-4S and 7C-12T-7L-3S also have  
483 posterior probabilities above 15%. Many primate taxa are polymorphic for 7C-13T-6L-3S and 7C-12T-  
484 7L-3S, which represent homeotic variants of each other: over one third of the taxa in our dataset that  
485 have 29 precaudal vertebrae are polymorphic for these two formulae. Given this pattern, it is very  
486 possible that ancestral primates were polymorphic for 7C-12T-7L-3S and 7C-13T-6L-3S as well. These  
487 results are consistent with previous work by Schultz and Straus (1945), Pilbeam (2004), and Williams  
488 (2011). This pattern appears to be retained at the base of haplorhines, anthropoids, platyrrhines, and  
489 catarrhines. The relatively high posterior probability for 7C-13T-6L-4S at the base of primates is more  
490 surprising since this formula is not particularly common among primates. However, the posterior  
491 probability for three sacral vertebrae in ancestral primates (67%) is over twice as high as that for four  
492 sacral vertebrae (32%). This fairly high posterior probability of four sacral vertebrae could represent  
493 polymorphism or merely uncertainty. Uncertainty in number of sacral vertebrae at the ancestral primate  
494 node is consistent with similar uncertainty seen at the roots of outgroup clades as well as the deep  
495 timespan and long branch lengths in that part of the tree.

496 Our analysis recovers substantial changes in vertebral numbers at the base of strepsirrhines and  
497 lorisiformes. Both lorisids and lemuriformes have increased numbers of presacral vertebrae relative to  
498 what we recover for the primate LCA, but galagids do not. In fact, the formula we recover for crown  
499 galagids is also our reconstructed ancestral primate formula. This means that additional presacral

500 vertebrae must either be convergent in lorises and lemuroids or that the formula of galagids represents a  
501 reversion to the ancestral primate condition. Our results recover the strongest support for the latter  
502 scenario. However, our taxon sample was not chosen to address this question. Since lorises are clearly  
503 derived in locomotor behavior and related postcranial morphology, including the vertebral column  
504 (Shapiro and Simons, 2002), it is possible that galagids, not lorises, represent the primitive loriseid (and  
505 potential strepsirrhine) condition. Additional research focused specifically on the evolution of vertebral  
506 numbers focused on strepsirrhines specifically may be useful to help parse this question.

507

#### 508 4.3. *The fossil record and vertebral evolution*

509 Ancestral state estimations using only extant taxa, as we have performed in this study, frequently  
510 fail to capture the full range of variation that existed throughout the evolutionary history of a clade, and  
511 the inclusion of fossils can improve on both ancestral character estimates and evolutionary models  
512 (Slater et al., 2012; Monson et al., 2022). This lack of fossil data represents a clear limitation of our  
513 study. Unfortunately, no fossils are complete enough to allow their inclusion in our analyses. Even the  
514 most complete fossil primate ever discovered, *Darwinius masillae*, does not include a complete vertebral  
515 column such that the total, precaudal, or presacral numbers of vertebrae are known (Franzen et al.,  
516 2009). Additionally, since many primate taxa are polymorphic, a single specimen is insufficient to  
517 capture the full range of variation or even the mode of that species' vertebral formula. Further, the  
518 phylogenetic placement of many fossil taxa is uncertain, complicating their inclusion.

519 Thompson and Alméjida's (2017) ancestral state reconstruction, however, was able to include  
520 limited fossil taxa due to the fact that they looked at vertebral segments independently, and there are  
521 several fossils that preserve whole or nearly whole segments of the vertebral column. Their results were  
522 broadly similar to ours—most of their analyses supported a  $LCA_{H-P}$  with four lumbar vertebrae (short  
523 back model), some with five (intermediate back model), and almost none with six (long back model).  
524 They accounted for uncertainty by running multiple iterations and making different assumptions about

525 each fossil (e.g., the placement of *Oreopithecus* as a stem or crown hominoid; the presence of five, six,  
526 or seven lumbar vertebrae in *Ekembo*; etc.). Despite the inclusion of fossils, however, they consistently  
527 found very little, if any support for the long back model. Even with the most generous assumptions  
528 possible about fossil taxa—six lumbar vertebrae in both *Ardipithecus ramidus* (for which only one  
529 lumbar vertebra has been published; Simpson et al., 2019) and *Australopithecus*, and six or seven  
530 lumbar vertebrae in *Ekembo* and *Nacholapithecus*, support for a  $LCA_{H-P}$  with six lumbar vertebrae was  
531 always less than 50% and usually much lower. And to produce even this modest support, all of these  
532 assumptions were required (e.g., when *Ardipithecus* is assumed to have six lumbar vertebrae, but  
533 *Australopithecus* is assumed to have five and *Ekembo* and *Nacholapithecus* are assumed to have six,  
534 support for the long back model is still <1%; see Thompson and Alméjida [2017] SOM Fig. S60).

535         In addition to the long back model requiring multiple improbable assumptions to receive even  
536 modest support, Thompson and Alméjida's (2017) inclusion of fossils and the resulting increase in  
537 uncertainty in phylogenetic relatedness may have represented an additional, inherent bias in favor of the  
538 long back model. Simulations have shown that when there is high uncertainty in phylogenetic trees,  
539 ancestral state reconstructions tend to recover more independent origins of traits (Duchêne and Lanfear,  
540 2015). The long back model requires a shorter back to evolve repeatedly in extant great apes (Fig. 1).  
541 Overall, both formal ancestral state reconstruction analyses performed to date have found the strongest  
542 support for the short back model and effectively no support for the long back model, despite using  
543 different approaches—Thompson and Alméjida (2017) included fossils but could not include a method  
544 that accounted for homeotic changes, while we utilized a method that accounts for both homeotic and  
545 meristic change but could not include fossils.

546

#### 547 4.4. *Comparisons with known fossils*

548         Although we do not include fossils in our study due to their incompleteness, we consider partial  
549 fossil vertebral columns here, allowing an independent test of hypotheses generated by our study.

550 The most complete primate fossil so far discovered, *Darwinius masillae*, includes complete  
551 cervical (7C), lumbar (7L), sacral (3S), and caudal (31) regions, but the thoracic column is incomplete,  
552 and it is stated that “11 thoracic vertebrae are present although their exact number is difficult to  
553 determine and therefore somewhat ambiguous” (Franzen et al., 2009:12). The phylogenetic position of  
554 *Darwinius* is subject to some debate (Franzen et al., 2009; Gingerich et al., 2010; Williams et al., 2010),  
555 although a position as a stem strepsirrhine seems likely (Williams et al., 2010). Seven cervical vertebrae,  
556 seven lumbar vertebrae, three sacral vertebrae, and greater than 11 thoracic vertebrae in a stem  
557 strepsirrhine is consistent with our results.

558 Other fossil primates are less complete. The stem catarrhine *Epipliopithecus vindobonensis* is  
559 missing vertebrae from both thoracic and lumbar regions (Zapfe, 1958) and, therefore cannot be used to  
560 address issues such as the 12T–7L vs 13T–6L configuration at the crown catarrhine or haplorhine nodes.  
561 Similarly, although numerous Miocene ape partial skeletons are known, only three species preserve  
562 more than several vertebrae: *Ekembo nyanzae*, *Nacholapithecus kerioi*, and *Oreopithecus bambolii*  
563 (Nakatsukasa, 2019). *Ekembo* and *Nacholapithecus* likely possessed 5–7 lumbar vertebrae and do not  
564 preserve complete sacra (Ward, 1993; Nakatsukasa, 2019; Hammond et al., 2020). Given their likely  
565 position as stem hominoids (Pugh, 2022), possessing 5–7 lumbar vertebra is consistent with a reduction  
566 from (perhaps polymorphic) six or seven lumbar vertebrae at the crown catarrhine node to five lumbar  
567 vertebrae at the crown hominoid node. The Bac#50 specimen of *Oreopithecus* does preserve a mostly  
568 complete sacrum consisting of six elements (but see Haeusler et al., 2002), but it is a different individual  
569 from the partial skeleton IGF 11778, which preserves five lumbar vertebrae, and the number of thoracic  
570 vertebrae in *Oreopithecus* is unknown (Straus, 1963; Nakatsukasa, 2019; Hammond et al., 2020;  
571 Nakatsukasa, 2019). The phylogenetic position of *Oreopithecus* is highly uncertain (Hammond et al.,  
572 2020; Pugh, 2022), but five lumbar vertebrae are consistent with a position as a stem hominoid or early-  
573 diverging crown hominoid. A six-element sacrum in *Oreopithecus* is more difficult to reconcile with our  
574 analyses unless it is a crown hominid, a placement considered highly unlikely (Harrison, 1987;



575 Hammond et al., 2020; Pugh, 2022), but this could also represent one of its many autapomorphies  
576 (Delson, 1986). Regardless, a long sacrum is most consistent with the short back model, consistent with  
577 our findings. Unfortunately, potential stem and crown hominids are known from no or too few vertebrae  
578 to hypothesize their regional vertebral configurations (Nakatsukasa, 2008, 2019; Susanna et al., 2010,  
579 2014; Nakatsukasa, 2008, 2019).

580 Fossil hominins are similarly incomplete, with no single skeleton or species known from  
581 complete thoracic, lumbar, and sacral regions (Meyer and Williams, 2019; Williams and Meyer, 2019;  
582 Machnicki and Reno, 2020), with the exception of Neandertals (Trinkaus, 1983; Arensburg, 1991; Rak,  
583 1991). Regional numbers are known (but sometimes debated) from single individuals in  
584 *Australopithecus afarensis* (thoracic and sacral: Russo and Williams, 2015; Machnicki et al., 2016a;  
585 Williams and Russo, 2016; Ward et al., 2017), *Australopithecus sediba* (lumbar and sacral: Williams et  
586 al., 2013, 2018, 2021), *Australopithecus africanus* (lumbar: Haeusler et al., 2002; Rosenman, 2008;  
587 Ward et al., 2020), and *Homo erectus* (lumbar and sacral: Haeusler et al., 2002; Schiess and Haeusler,  
588 2013). It has been inferred based on comparative work that *Ardipithecus ramidus* may have possessed  
589 six lumbar vertebrae (Lovejoy et al., 2009; McCollum et al., 2010; but see Williams and Pilbeam, 2021),  
590 which would be at odds with our analysis here. Only one lumbar fragment of *Ardipithecus ramidus* is  
591 currently known and was not discovered with the original material at Aramis (Simpson et al., 2019).

592 Only one Neanderthal preserves a nearly complete precaudal column from which to confidently  
593 infer vertebral formula, Kebara 2 (Arensburg, 1991). Kebara 2 may have the same vertebral  
594 configuration as modern humans do modally (7C-12T-5L-5S), but the first lumbar vertebra bears riblets  
595 ('lumbar ribs') rather than typical costal (lumbar transverse) processes (Ogilvie et al., 1998). Another  
596 partial skeleton, Shanidar 3, preserves a few cervical vertebrae, many thoracic vertebrae along with all  
597 elements of the lumbar column and sacrum (Trinkaus, 1983 1983, 2018; Gómez-Olivencia et al., 2013a;  
598 Trinkaus, 2018). Shanidar 3's thoracolumbar transition additionally includes evidence for a caudal shift  
599 in vertebral identity: what is frequently referred to as the first lumbar vertebra bears large costal facets

600 on the pedicles (Ogilvie et al., 1998). In both cases (Kebara 2 and Shanidar 3), the criteria established by  
601 Schultz and employed in this study would identify four lumbar vertebrae and 13 thoracic vertebrae in the  
602 case of Kebara 2 (and also likely Shanidar 3). Other nearly complete Neandertal specimens such as La  
603 Chapelle-aux-Saints 1 and Regourdou 1 seem to conform to the modal modern human pattern of 7C-  
604 12T-5L (Gómez-Olivencia, 2013; Gómez-Olivencia et al., 2013b), but individual thoracic and lumbar  
605 vertebrae are missing, and only the upper sacrum is present in both individuals, precluding assessment of  
606 sacral vertebra composition. We did not include Neandertals or other fossils hominins in our analysis for  
607 these reasons but note that vertebral counts in these fossils are not inconsistent with the short-back  
608 model. This is especially true given the high degree of polymorphism observed in extant hominoid taxa,  
609 including humans (which frequently possess 6S; Williams et al., 2019a). Overall, then, although the lack  
610 of fossil data in the ancestral state reconstruction represents a clear limitation of this study, no known  
611 fossils contradict our results.

612

## 613 **5. Conclusions**

614 We performed formal ancestral state reconstructions of the number of vertebrae in primates  
615 based on extant taxa and taking into account both homeotic and meristic changes in the vertebral  
616 column. We find strong support for the short back model of ape and human evolution. The long back  
617 model is rejected by our analyses. The intermediate back model receives little support but cannot be  
618 rejected. Our results are necessarily based on extant taxa but are not contradicted by any known fossils.  
619 Until potentially contradictory fossil material is discovered, the best-supported hypothesis for the  
620 numerical configuration of the vertebral column of the  $LCA_{H-P}$  is the short back model. Complete  
621 understanding of the contribution of the lower back to positional behavior of the  $LCA_{H-P}$  requires  
622 reconstruction of the location of the transitional vertebra (Shapiro, 1993; Russo, 2010; Williams, 2012b,  
623 c; Williams et al., 2013, 2016, 2019a; Williams and Russo, 2015; Thompson and Almécija, 2017; Ward  
624 et al., 2017; Nalley et al., 2019; but see Haeusler et al., 2011, 2012), which is beyond the scope of this

625 study. However, a short-backed ancestor is most consistent with great ape-like posture and locomotion;  
626 namely, orthograde and probably forelimb-dominated suspensory behaviors in trees and quadrupedal  
627 locomotion on the ground. Future recovery and study of fossil material will test hypotheses on the nature  
628 of the LCA<sub>H-P</sub>. Specifically, vertebrae from Miocene and early Pliocene hominins, members of the *Pan*  
629 or *Gorilla* lineage, or stem hominines will allow us to more thoroughly test the hypothesis of an African  
630 ape-like vertebral formula in the LCA<sub>H-P</sub>.

631

### 632 **Acknowledgments**

633 We thank N. Duncan, G. Garcia, E. Hoeger, S. Ketelsen, A. Marcato, B. O’Toole, M. Surovy, E.  
634 Westwig (American Museum of Natural History); M. Milella, M. Ponce de León, C. Zollikofer,  
635 (Anthropological Institute and Museum, University of Zurich); Y. Haile-Selassie, L. Jellema (Cleveland  
636 Museum of Natural History); H. Taboada (Department of Anthropology, New York University); D. Katz,  
637 T. Weaver, (Department of Anthropology, U.C. Davis); B. Patterson, A. Goldman, M. Schulenberg, L.  
638 Smith, W. Stanley (Field Museum of Natural History); C. McCaffery, D. Reed (Florida Museum of  
639 Natural History, University of Florida); J. Chupasko, J. Harrison, M. Omura (Harvard Museum of  
640 Comparative Zoology); E. Gilissen, W. Wendelen (Musée Royal de l’Afrique Centrale); S. Jancke, N.  
641 Lange, F. Mayer, (Museum für Naturkunde, Berlin); C. Conroy (Museum of Vertebrate Zoology, U.C.  
642 Berkeley); N. Edminion, L. Gordon, K. Helgen, E. Langan, D. Lunde, J. Ososky, R. Thorington  
643 (National Museum of Natural History, Smithsonian Institution); J. Soderberg, M. Tappen (Neil C.  
644 Tappen Collection, University of Minnesota); S. Bruaux, G. Lenglet (Royal Belgian Institute of Natural  
645 Sciences); M. Hiermeier (Zoologische Staatssammlung München); B. Wilkey and I. Livne (Powell-  
646 Cotton Museum, Birchington); C. Lefèvre (Muséum national d’Histoire naturelle; Paris); D. Grimaud-  
647 Hervé, A. Fort, V. Laborde, L. Huet (Musée de l’Homme, Paris); R. Portela (Natural History Museum,  
648 London), J. Stock, M. Mirazón Lahr (Duckworth Collection, University of Cambridge); A. Rodríguez-  
649 Hidalgo (Institut Català de Paleoecologia Humana i Evolució Social, Tarragona); the Grant Museum of

650 Zoology, University College of London; and the Oxford University Museum of Natural History for  
651 facilitating access to specimens in their care. We thank S. McFarlin for granting us access to images of  
652 mountain gorilla specimens, and we are grateful to the Rwandan government for permission to study  
653 Virunga mountain gorilla skeletal specimens from the Volcanoes National Park curated by the Mountain  
654 Gorilla Skeletal Project, established through the continuous efforts of researchers and staff of the  
655 Rwanda Development Board's Department of Tourism and Conservation, Dian Fossey Gorilla Fund,  
656 Gorilla Doctors, Institute of National Museums of Rwanda, The George Washington University, and  
657 New York University College of Dentistry, and funding by the National Science Foundation (BCS-  
658 0852866, BCS-0964944, BCS-1520221), National Geographic Society's Committee for Research and  
659 Exploration (8486-08), and The Leakey Foundation. J.K.S. was funded through the National Science  
660 Foundation (BCS-2041700), the Leakey Foundation, and Sigma Xi. S.A.W. was funded through the  
661 National Science Foundation (BCS-0925734), the Leakey Foundation, and the New York University  
662 Research Challenge Fund. A.G.-O. was funded by two Synthesys grants (GB-TAF-3674, BE-TAF-4132)  
663 and a Marie Curie fellowship (MC-IEF 327243) funded by the European commission, a Ramón y Cajal  
664 fellowship by the Ministerio de Ciencia, Innovación y Universidades (RYC-2017-22558), the Grupo  
665 IT1485-22 from the Gobierno Vasco/Eusko Jaurlaritz, and the Ministerio de Ciencia e Innovación  
666 (project PID2021-122355NB-C31).

667

## 668 **References**

669

- 670 Arensburg, B., 1991. The vertebral column, thoracic cage and hyoid bone. In: Bar-Yosef, O. (Ed.), *Le*  
671 *Squelette Moustérien de Kébara*. Éditions du CNRS, Paris, pp. 113–147.
- 672 Arnold, C., Matthews, L.J., Nunn, C.L., 2010. The 10kTrees website: A new online resource for primate  
673 phylogeny. *Evol. Anthropol.* 19, 114–118.

674 Bininda-Emonds, O.R.P., Cardillo, M., Jones, K.E., MacPhee, R.D.E., Beck, R.M.D., Grenyer, R., Price,  
675 S.A., Vos, R.A., Gittleman, J.L., Purvis, A., 2007. The delayed rise of present-day mammals.  
676 Nature 446, 507–512.

677 Bollback, J.P., 2006. SIMMAP: Stochastic character mapping of discrete traits on phylogenies. BMC  
678 Bioinform. 7, 88.

679 Carapuço, M., Nóvoa, A., Bobola, N., Mallo, M., 2005. Hox genes specify vertebral types in the  
680 presomitic mesoderm. Genes Dev. 19, 2116–2121.

681 Clausier, D.A., 1980. Functional and comparative anatomy of the primate spinal column: Some  
682 locomotor and postural adaptations. Ph.D. Dissertation, University of Wisconsin–Milwaukee.

683 Davis, A.P., Capecchi, M.R., 1994. Axial homeosis and appendicular skeleton defects in mice with a  
684 targeted disruption of *hoxd-11*. Development 120, 2187–2198.

685 Delson, E., 1986. An anthropoid enigma: Historical introduction to the study of *Oreopithecus bambolii*.  
686 J. Hum. Evol. 15, 523–531.

687 Duchêne, S., Lanfear, R., 2015. Phylogenetic uncertainty can bias the number of evolutionary transitions  
688 estimated from ancestral state reconstruction methods. J. Exp. Zool. B Mol. Dev. Evol. 324, 517–  
689 524.

690 Favier, B., Le Meur, M., Chambon, P., Dollé, P., 1995. Axial skeleton homeosis and forelimb  
691 malformations in *Hoxd-11* mutant mice. Proc. Natl. Acad. Sci. USA 92, 310–314.

692 Franzen, J.L., Gingerich, P.D., Habersetzer, J., Hurum, J.H., Koenigswald, W. von, Smith, B.H., 2009.  
693 Complete primate skeleton from the Middle Eocene of Messel in Germany: Morphology and  
694 paleobiology. PLoS One 4, e5723.

695 Fulwood, E.L., O’Meara, B.C., 2014. A phylogenetic approach to the evolution of anthropoid lumbar  
696 number. Am. J. Phys. Anthropol. 153, 123–123.

697 Galis, F., 1999a. Why do almost all mammals have seven cervical vertebrae? Developmental constraints,  
698 Hox genes, and cancer. J. Exp. Zool. 285, 19–26.

699 Galis, F., 1999b. On the homology of structures and Hox genes: The vertebral column. In: Bock, G.,  
700 Cardew, G. (Eds.), Novartis Foundation Symposium 222 – Homology. John Wiley & Sons, Ltd,  
701 Chichester, pp. 80–94.

702 Galis, F., Carrier, D.R., Alphen, J. van, Mije, S.D. van der, Dooren, T.J.M.V., Metz, J.A.J., Broek,  
703 C.M.A. 2014. Fast running restricts evolutionary change of the vertebral column in mammals.  
704 Proc. Natl. Acad. Sci. USA 111, 11401–11406.

705 Gingerich, P.D., Franzen, J.L., Habersetzer, J., Hurum, J.H., Smith, B.H., 2010. *Darwinius masillae* is a  
706 Haplorhine — Reply to Williams et al. (2010). J. Hum. Evol. 59, 574–579.

707 Gómez-Olivencia, A., 2013. Back to the old man’s back: Reassessment of the anatomical determination  
708 of the vertebrae of the Neandertal individual of La Chapelle-aux-Saints. Ann. Paléontol. 99, 43–  
709 65.

710 Gómez-Olivencia, A., Been, E., Arsuaga, J.L., Stock, J.T., 2013a. The Neandertal vertebral column 1:  
711 The cervical spine. J. Hum. Evol. 64, 608–630.

712 Gómez-Olivencia, A., Couture-Veschambre, C., Madelaine, S., Maureille, B., 2013b. The vertebral  
713 column of the Regourdou 1 Neandertal. J. Hum. Evol. 64, 582–607.

714 Haeusler, M., Martelli, S.A., Boeni, T., 2002. Vertebrae numbers of the early hominid lumbar spine. J.  
715 Hum. Evol. 43, 621–643.

716 Haeusler, M., Schiess, R., Boeni, T., 2011. New vertebral and rib material point to modern bauplan of  
717 the Nariokotome *Homo erectus* skeleton. J. Hum. Evol. 61, 575–582.

718 Haeusler, M., Schiess, R., Böni, T., 2012. Modern or distinct axial bauplan in early hominins? A reply to  
719 Williams (2012) J. Hum. Evol. 63, 557–559.

720 Hammond, A.S., Rook, L., Anaya, A.D., Cioppi, E., Costeur, L., Moyà-Solà, S., Almécija, S., 2020.  
721 Insights into the lower torso in late Miocene hominoid *Oreopithecus bambolii*. Proc. Natl. Acad.  
722 Sci. USA 117, 278–284.

723 Harrison, T., 1987. A reassessment of the phylogenetic relationships of *Oreopithecus bambolii* Gervais.  
724 J. Hum. Evol. 15, 541–583.

725 Johanson, D.C., Lovejoy, C.O., Kimbel, W.H., White, T.D., Ward, S.C., Bush, M.E., Latimer, B.M.,  
726 Coppens, Y., 1982. Morphology of the Pliocene partial hominid skeleton (A.L. 288-1) from the  
727 Hadar formation, Ethiopia. Am. J. Phys. Anthropol. 57, 403–451.

728 Latimer, B.M., Ward, C.V., 1993. The thoracic and lumbar vertebrae. In: Walker, A.C., Leakey, R. (Eds.),  
729 The Narikotome *Homo Erectus*. Harvard University Press, Cambridge, pp. 266–293.

730 Lewis, P.O., 2001. A likelihood approach to estimating phylogeny from discrete morphological character  
731 data. Syst. Biol. 50, 913–925.

732 Lovejoy, C.O., 2005. The natural history of human gait and posture: Part 2. Hip and thigh. Gait Posture  
733 21, 113–124.

734 Lovejoy, C.O., McCollum, M.A., 2010. Spinopelvic pathways to bipedality: Why no hominids ever  
735 relied on a bent-hip–bent-knee gait. Philos. Trans. R. Soc. B Biol. Sci. 365, 3289–3299.

736 Lovejoy, C.O., Suwa, G., Simpson, S.W., Matternes, J.H., White, T.D., 2009. The great divides:  
737 *Ardipithecus ramidus* reveals the postcrania of our last common ancestors with African apes.  
738 Science 326, 73–106.

739 MacArthur, R.H., 1957. On the relative abundance of bird species. Proc. Natl. Acad. Sci. USA 43, 293–  
740 295.

741 Machnicki, A.L., Lovejoy, C.O., Reno, P.L., 2016. Developmental identity versus typology: Lucy has  
742 only four sacral segments. Am. J. Phys. Anthropol. 160, 729–739.

743 Machnicki, A.L., Reno, P.L., 2020. Great apes and humans evolved from a long-backed ancestor. J.  
744 Hum. Evol. 144, 102791.

745 Mallo, M., Wellik, D.M., Deschamps, J., 2010. Hox genes and regional patterning of the vertebrate Body  
746 plan. Dev. Biol. 344, 7–15.

747 McCollum, M.A., Rosenman, B.A., Suwa, G., Meindl, R.S., Lovejoy, C.O., 2010. The vertebral formula  
748 of the last common ancestor of African apes and humans. *J. Exp. Zool. B Mol. Dev. Evol.* 314B,  
749 123–134.

750 McIntyre, D.C., Rakshit, S., Yallowitz, A.R., Loken, L., Jeannotte, L., Capecchi, M.R., Wellik, D.M.,  
751 2007. Hox patterning of the vertebrate rib cage. *Development* 134, 2981–2989.

752 Meyer, M.R., Williams, S.A., 2019. The spine of Early Pleistocene *Homo*. In: Been, E., Gómez-  
753 Olivencia, A., Ann Kramer, P. (Eds.), *Spinal Evolution: Morphology, Function, and Pathology of*  
754 *the Spine in Hominoid Evolution*. Springer International Publishing, Cham, pp. 153–183.

755 Monson, T.A., Brasil, M.F., Mahaney, M.C., Schmitt, C.A., Taylor, C.E., Hlusko, L.J., 2022. Keeping  
756 21st century paleontology grounded: Quantitative genetic analyses and ancestral state  
757 reconstruction re-emphasize the essentiality of fossils. *Biology* 11, 1218.

758 Nakatsukasa, M., 2008. Comparative study of Moroto vertebral specimens. *J. Hum. Evol.* 55, 581–588.

759 Nakatsukasa, M., 2019. Miocene ape spinal morphology: The evolution of orthogrady. In: Been, E.,  
760 Gómez-Olivencia, A., Ann Kramer, P. (Eds.), *Spinal Evolution: Morphology, Function, and*  
761 *Pathology of the Spine in Hominoid Evolution*. Springer International Publishing, Cham, pp. 73–  
762 96.

763 Nakatsukasa, M., Tsujikawa, H., Shimizu, D., Takano, T., Kunimatsu, Y., Nakano, Y., Ishida, H., 2003.  
764 Definitive evidence for tail loss in *Nacholapithecus*, an East African Miocene hominoid. *J. Hum.*  
765 *Evol.* 45, 179–186.

766 Nakatsukasa, M., Ward, C.V., Walker, A., Teaford, M.F., Kunimatsu, Y., Ogihara, N., 2004. Tail loss in  
767 *Proconsul heseloni*. *J. Hum. Evol.* 46, 777–784.

768 Nalley, T.K., Scott, J.E., Ward, C.V., Alemseged, Z., 2019. Comparative morphology and ontogeny of  
769 the thoracolumbar transition in great apes, humans, and fossil hominins. *J. Hum. Evol.* 134,  
770 102632.



771 Narita, Y., Kuratani, S., 2005. Evolution of the vertebral formulae in mammals: A perspective on  
772 developmental constraints. *J. Exp. Zool. B Mol. Dev. Evol.* 304B, 91–106.

773 Ogilvie, M.D., Hilton, C.E., Ogilvie, C.D., 1998. Lumbar anomalies in the Shanidar 3 Neandertal. *J.*  
774 *Hum. Evol.* 35, 597–610.

775 Pilbeam, D., 2004. The anthropoid postcranial axial skeleton: Comments on development, variation, and  
776 evolution. *J. Exp. Zool. B Mol. Dev. Evol.* 302B, 241–267.

777 Plummer, M., Best, N., Cowles, K., Vines, K., 2006. CODA: Convergence diagnosis and output analysis  
778 for MCMC. *R News* 6, 7–11.

779 Pugh, K.D., 2022. Phylogenetic analysis of Middle-Late Miocene apes. *J. Hum. Evol.* 165, 103140.

780 R Core Team, 2022. R: A language and environment for statistical computing. R foundation for  
781 statistical computing. Vienna, Austria.

782 Rak, Y., 1991. The pelvis. In: Bar-Yosef, O. (Ed.), *Le Squelette Moustérien de Kébara*. Editions du  
783 CNRS, Paris, pp. 147–156.

784 Revell, L.J., 2012. phytools: An R package for phylogenetic comparative biology (and other things).  
785 *Methods Ecol. Evol.* 3, 217–223.

786 Rosenman, B., 2008. Triangulating the evolution of the vertebral column in the last common ancestor:  
787 Thoracolumbar transverse process homology in the Hominoidea. Ph.D. Dissertation, Kent State  
788 University.

789 Russo, G.A., 2010. Prezygapophyseal articular facet shape in the catarrhine thoracolumbar vertebral  
790 column. *Am. J. Phys. Anthropol.* 142, 600–612.

791 Russo, G.A., 2015. Postsacral vertebral morphology in relation to tail length among primates and other  
792 mammals. *Anat. Rec.* 298, 354–375.

793 Russo, G.A., 2016. Comparative sacral morphology and the reconstructed tail lengths of five extinct  
794 primates: *Proconsul heseloni*, *Epipliopithecus vindobonensis*, *Archaeolemur edwardsi*,  
795 *Megaladapis grandidieri*, and *Palaeopropithecus kelyus*. *J. Hum. Evol.* 90, 135–162.

- 796 Russo, G.A., Williams, S.A., 2015. “Lucy” (A.L. 288-1) had five sacral vertebrae. *Am. J. Phys.*  
797 *Anthropol.* 156, 295–303.
- 798 Schiess, R., Haeusler, M., 2013. No skeletal dysplasia in the nariokotome boy KNM-WT 15000 (*Homo*  
799 *erectus*)—A reassessment of congenital pathologies of the vertebral column. *Am. J. Phys.*  
800 *Anthropol.* 150, 365–374.
- 801 Schultz, A.H., 1950. The physical distinctions of Man. *Proc. Am. Philos. Soc.* 94, 428–449.
- 802 Schultz, A.H., 1961. Vertebral column and thorax. *Primatologia* 4, 1–66.
- 803 Schultz, A.H., Straus, W.L., 1945. The numbers of vertebrae in primates. *Proc. Am. Philos. Soc.* 89,  
804 601–626.
- 805 Shapiro, L., 1993. Functional morphology of the vertebral column in primates. In: Gebo, D.L. (Ed.),  
806 *Postcranial Adaptation in Non-Human Primates*. Northern Illinois University Press, Dekalb, pp.  
807 121–149.
- 808 Shapiro, L.J., Kemp, A.D., 2019. Functional and developmental influences on intraspecific variation in  
809 catarrhine vertebrae. *Am. J. Phys. Anthropol.* 168, 131–144.
- 810 Shapiro, L.J., Simons, C.V.M., 2002. Functional aspects of strepsirrhine lumbar vertebral bodies and  
811 spinous processes. *J. Hum. Evol.* 42, 753–783.
- 812 Simpson, S.W., Levin, N.E., Quade, J., Rogers, M.J., Semaw, S., 2019. *Ardipithecus ramidus* postcrania  
813 from the Gona Project area, Afar Regional State, Ethiopia. *J. Hum. Evol.* 129, 1–45.
- 814 Slater, G.J., Harmon, L.J., Alfaro, M.E., 2012. Integrating fossils with molecular phylogenies improves  
815 inference of trait evolution: Fossils, phylogenies, and models of trait evolution. *Evolution* 66,  
816 3931–3944.
- 817 Springer, M.S., Meredith, R.W., Gatesy, J., Emerling, C.A., Park, J., Rabosky, D.L., Stadler, T., Steiner,  
818 C., Ryder, O.A., Janečka, J.E., Fisher, C.A., Murphy, W.J., 2012. Macroevolutionary dynamics  
819 and historical biogeography of primate diversification inferred from a species supermatrix. *PLoS*  
820 *One* 7, e49521.

- 821 Straus, W.L., 1963. The classification of *Oreopithecus*. In: Washburn, S.L. (Ed.), Classification and  
822 Human Evolution. Routledge, London, pp. 146–177.
- 823 Susanna, I., Alba, D.M., Almécija, S., 2010. Las vertebrae lumbares del gran simio antropomorfo basal  
824 del Mioceno Medio *Pierolapithecus catalaunicus* (Primates: Hominidae). *Cidaris* 30, 311–316.
- 825 Susanna, I., Alba, D.M., Almécija, S., Moyà-Solà, S., 2014. The vertebral remains of the late Miocene  
826 great ape *Hispanopithecus laietanus* from Can Llobateres 2 (Vallès-Penedès Basin, NE Iberian  
827 Peninsula). *J. Hum. Evol.* 73, 15–34.
- 828 Tague, R.G., 2017. Sacral variability in tailless species: *Homo sapiens* and *Ochotona princeps*. *Anat.*  
829 *Rec.* 300, 798–809.
- 830 Tardieu, C., Haeusler, M., 2019. The acquisition of human verticality with an emphasis on sagittal  
831 balance. In: Roussouly, P., Pinheiro-Franco, J.L., Labelle, H., Gehrechen, M. (Eds.), *Sagittal*  
832 *Balance of the Spine*. Thieme Publishers, New York, pp. 13–22.
- 833 Thompson, N.E., Almécija, S., 2017. The evolution of vertebral formulae in Hominoidea. *J. Hum. Evol.*  
834 110, 18–36.
- 835 Trinkaus, E., 1983. *The Shanidar Neandertals*. Academic Press, Cambridge.
- 836 Trinkaus, E., 2018. An abundance of developmental anomalies and abnormalities in Pleistocene people.  
837 *Proc. Natl. Acad. Sci. USA.* 115, 11941–11946.
- 838 Upham, N.S., Esselstyn, J.A., Jetz, W., 2019. Inferring the mammal tree: Species-level sets of  
839 phylogenies for questions in ecology, evolution, and conservation. *PloS Biol.* 17, e3000494.
- 840 Wahba, G.M., Hostikka, S.L., Carpenter, E.M., 2001. The paralogous Hox genes *Hoxa10* and *Hoxd10*  
841 interact to pattern the mouse hindlimb peripheral nervous system and skeleton. *Dev. Biol.* 231,  
842 87–102.
- 843 Ward, C.V., 1993. Torso morphology and locomotion in *Proconsul nyanzae*. *Am. J. Phys. Anthropol.* 92,  
844 291–328.
- 845 Ward, C.V., Walker, A., Teaford, M.F., 1991. *Proconsul* did not have a tail. *J. Hum. Evol.* 21, 215–220.

846 Ward, C.V., Nalley, T.K., Spoor, F., Tafforeau, P., Alemseged, Z., 2017. Thoracic vertebral count and  
847 thoracolumbar transition in *Australopithecus afarensis*. Proc. Natl. Acad. Sci. USA 114, 6000–  
848 6004.

849 Ward, C.V., Rosenman, B., Latimer, B.M., Nalla, S., 2020. Thoracolumbar vertebrae and ribs. In: Zipfel,  
850 B., Richmond, B.G., Ward, C.V. (Eds.), Hominin Postcranial Remains from Sterkfontein, South  
851 Africa, 1936-1995. Oxford University Press, Oxford, pp. 144–186.

852 Wellik, D.M., Capecchi, M.R., 2003. Hox10 and Hox11 genes are required to globally pattern the  
853 mammalian skeleton. Science 301, 363–367.

854 Whitcome, K.K., Shapiro, L.J., Lieberman, D.E., 2007. Fetal load and the evolution of lumbar lordosis  
855 in bipedal hominins. Nature 450, 1075–1078.

856 Williams, B.A., Kay, R.F., Kirk, E.C., Ross, C.F., 2010. *Darwinius masillae* is a strepsirrhine—a reply to  
857 Franzen et al. (2009). J. Hum. Evol. 59, 567–573.

858 Williams, S.A., 2011. Evolution of the hominoid vertebral column. Ph.D. Dissertation, University of  
859 Illinois at Urbana-Champaign.

860 Williams, S.A., 2012a. Variation in anthropoid vertebral formulae: Implications for homology and  
861 homoplasy in hominoid evolution. J. Exp. Zool. B Mol. Dev. Evol. 318, 134–147.

862 Williams, S.A., 2012b. Placement of the diaphragmatic vertebra in catarrhines: Implications for the  
863 evolution of dorsostability in hominoids and bipedalism in hominins. Am. J. Phys. Anthropol.  
864 148, 111–122.

865 Williams, S.A., 2012c. Modern or distinct axial bauplan in early hominins? Comments on Haeusler et al.  
866 (2011). J. Hum. Evol. 63, 552–556.

867 Williams, S.A., Gómez-Olivencia, A., Pilbeam, D.R., 2019a. Numbers of vertebrae in hominoid  
868 evolution. In: Been, E., Gómez-Olivencia, A., Ann Kramer, P. (Eds.), Spinal Evolution:  
869 Morphology, Function, and Pathology of the Spine in Hominoid Evolution. Springer  
870 International Publishing, Cham, pp. 97–124.

871 Williams, S.A., Meyer, M.R., 2019. The Spine of *Australopithecus*. In: Been, E., Gómez-Olivencia, A.,  
872 Ann Kramer, P. (Eds.), Spinal Evolution: Morphology, Function, and Pathology of the Spine in  
873 Hominoid Evolution. Springer International Publishing, Cham, pp. 125–151.

874 Williams, S.A., Meyer, M.R., Nalla, S., García-Martínez, D., Nalley, T.K., Eyre, J., Prang, T.C., Bastir,  
875 M., Schmid, P., Churchill, S.E., 2018. The vertebrae, ribs, and sternum of *Australopithecus*  
876 *sediba*. *PaleoAnthropology* 2018, 156–233.

877 Williams, S.A., Middleton, E.R., Villamil, C.I., Shattuck, M.R., 2016. Vertebral numbers and human  
878 evolution. *Am. J. Phys. Anthropol.* 159, 19–36.

879 Williams, S.A., Ostrofsky, K.R., Frater, N., Churchill, S.E., Schmid, P., Berger, L.R., 2013. The vertebral  
880 column of *Australopithecus sediba*. *Science* 340, 1232996.

881 Williams, S.A., Pilbeam, D., 2021. Homeotic change in segment identity derives the human vertebral  
882 formula from a chimpanzee-like one. *Am. J. Phys. Anthropol.* 176,283-294.

883 Williams, S.A., Prang, T.C., Meyer, M.R., Nalley, T.K., Van Der Merwe, R., Yelverton, C., García-  
884 Martínez, D., Russo, G.A., Ostrofsky, K.R., Spear, J., Eyre, J., Grabowski, M., Nalla, S., Bastir,  
885 M., Schmid, P., Churchill, S.E., Berger, L.R., 2021. New fossils of *Australopithecus sediba*  
886 reveal a nearly complete lower back. *eLife* 10, e70447.

887 Williams, S.A., Russo, G.A., 2015. Evolution of the hominoid vertebral column: The long and the short  
888 of it. *Evol. Anthropol.* 24, 15–32.

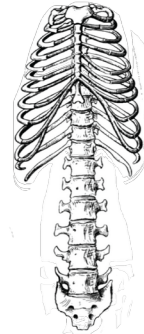
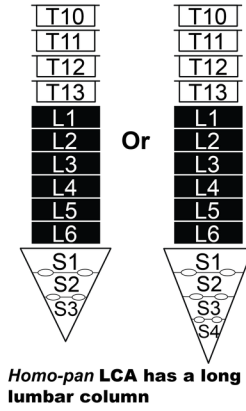
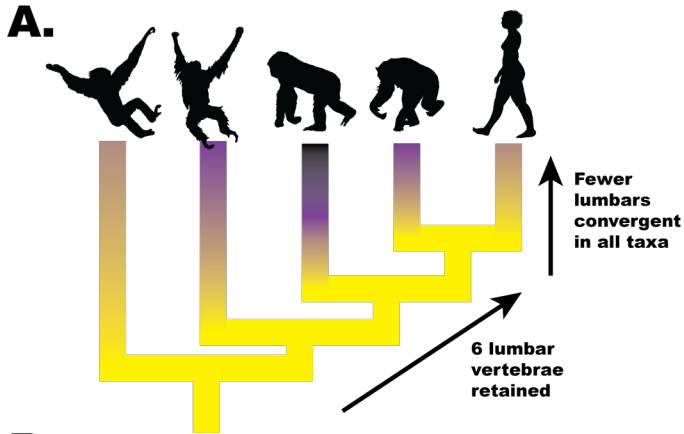
889 Williams, S.A., Russo, G.A., 2016. The fifth element (of Lucy’s sacrum): Reply to Machnicki, Lovejoy,  
890 and Reno. *Am. J. Phys. Anthropol.* 161, 374-378.

891 Williams, S.A., Spear, J.K., Petruccio, L., Goldstein, D.M., Lee, A.B., Peterson, A.L., Miano, D.A.,  
892 Kaczmarek, E.B., Shattuck, M.R., 2019b. Increased variation in numbers of presacral vertebrae  
893 in suspensory mammals. *Nat. Ecol. Evol.* 3, 949–956.

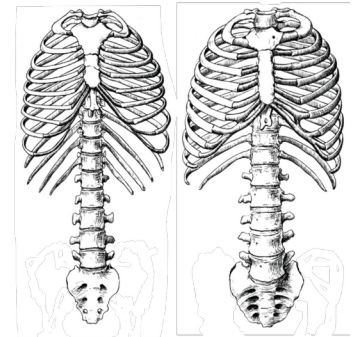
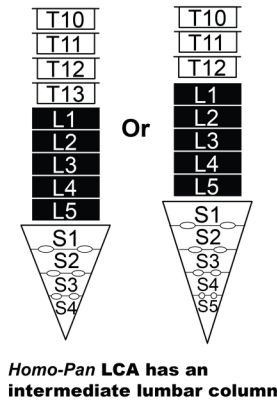
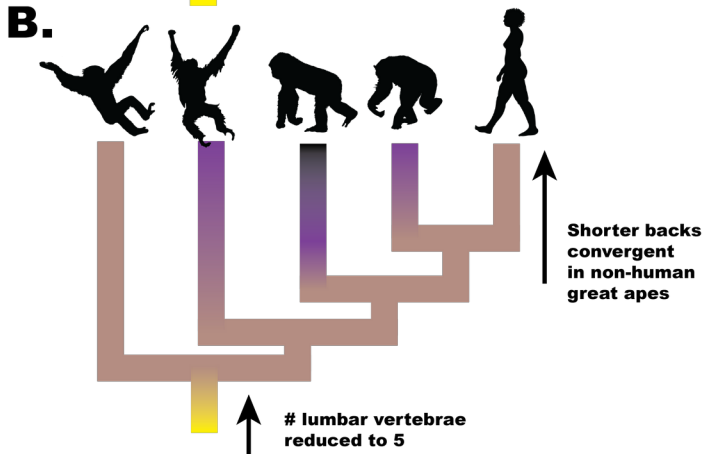
894 Williams, S.A., Zeng, I., Paton, G.J., Yelverton, C., Dunham, C., Ostrofsky, K.R., Shukman, S., Avilez,  
895 M.V., Eyre, J., Loewen, T., Prang, T.C., Meyer, M.R., 2022. Inferring lumbar lordosis in  
896 Neandertals and other hominins. Proc. Natl. Acad. Sci. Nexus 1, pgab005.

897 Zapfe, H., 1958. The skeleton of *Pliopithecus (Epipliopithecus) vindobonensis* Zapfe and Hürzeler. Am.  
898 J. Phys. Anthropol. 16, 441–457.

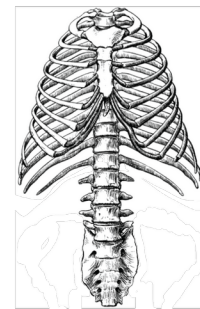
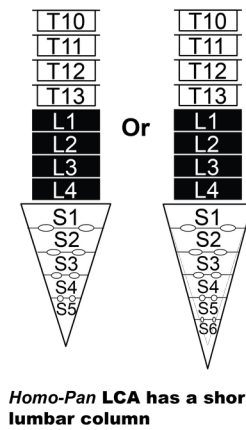
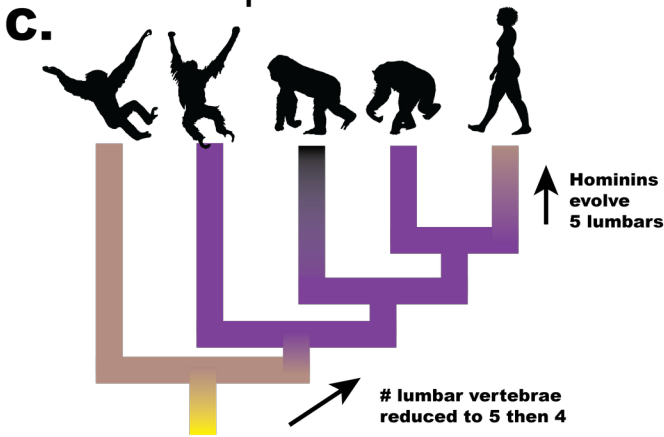
899



Extant example: Macaque



Extant examples: Gibbon (left), human (right)

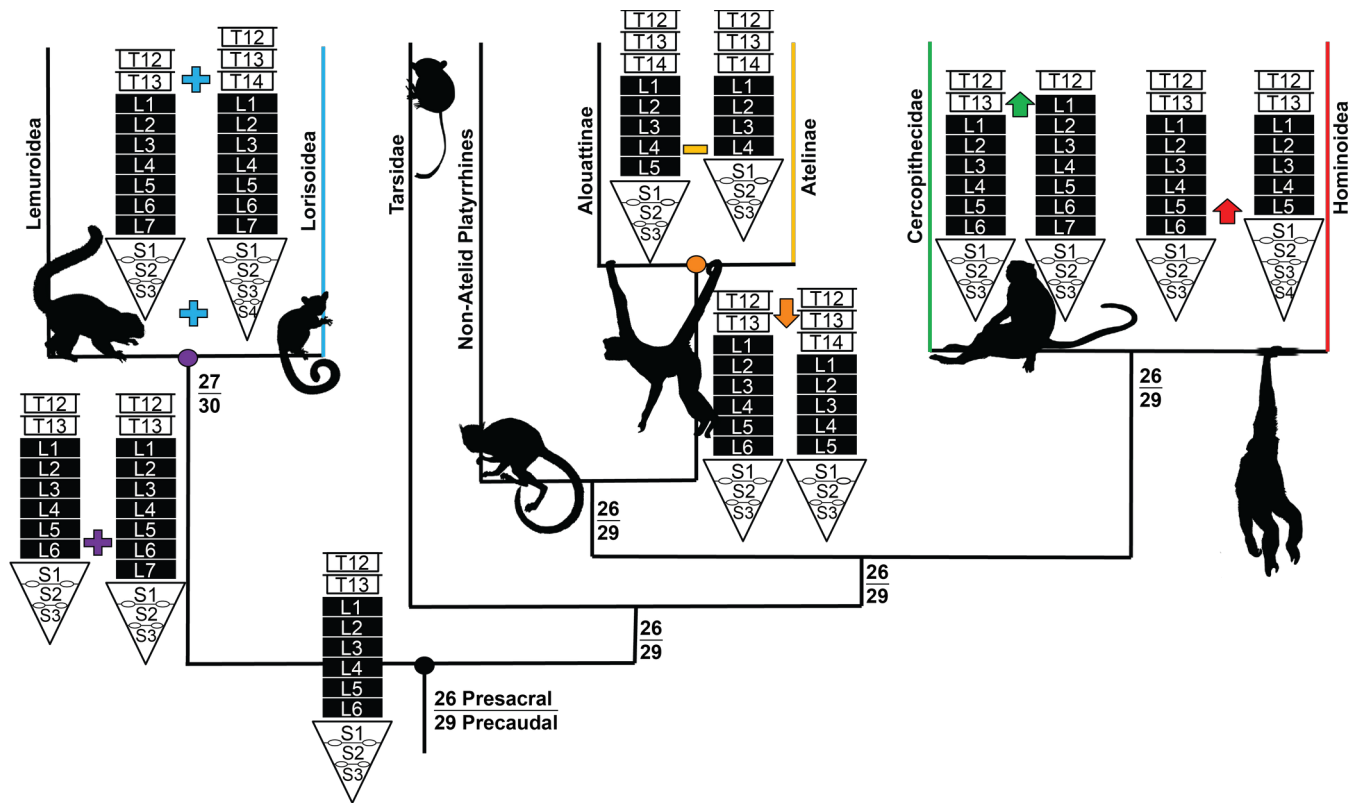


Extant example: Chimpanzee.

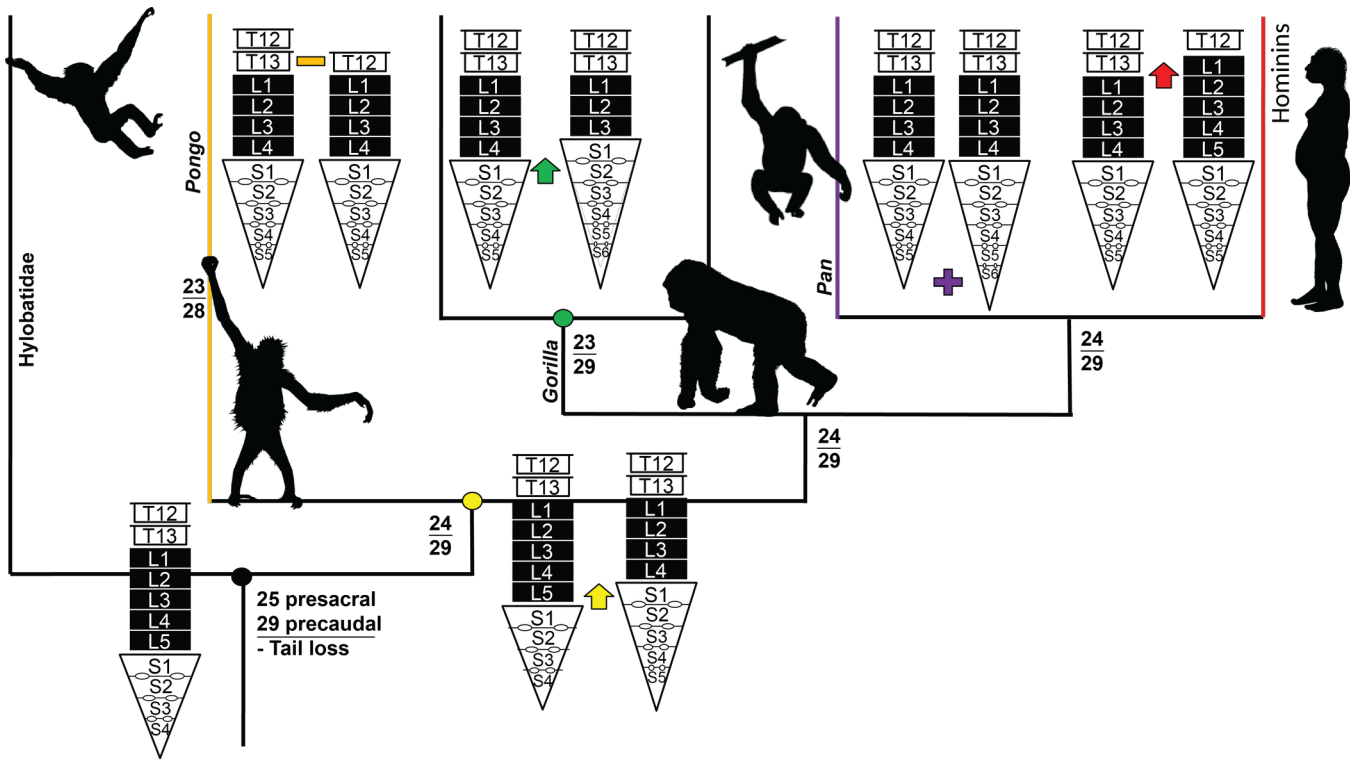


903 **Figure 1.** Visual representations of the different models for the last common ancestor of hominins and  
904 panins. A) Long back model, with 13 thoracic vertebrae, six lumbar vertebrae, and four sacral vertebrae.  
905 B) Intermediate back models, one with 13 thoracic vertebrae, five lumbar vertebrae, and four sacral  
906 vertebrae and the other with 12 thoracic vertebrae, five lumbar vertebrae, and five sacral vertebrae. C)  
907 Short back model, with 13 thoracic vertebrae, four lumbar vertebrae, and five sacral vertebrae.  
908 Illustrations modified from (Schultz, 1950). Silhouettes from PhyloPic.org.





910 **Figure 2.** Summary of results with highest posterior probabilities for major clades of primates (Order  
 911 Primates). The lower thoracic column, lumbar column, and sacrum are diagrammed ancestrally and on  
 912 each stem. Transitions are shown (plus symbol = meristic addition of an element; minus symbol =  
 913 meristic loss of an element; downward facing arrow = caudally-directed homeotic shift; upward facing  
 914 arrow = cranially-directed homeotic shift), and colors correspond to nodes and lineages (e.g., purple =  
 915 strepsirrhine node). Combined numbers of presacral (C + T + L) and precaudal (C + T + L + S) are listed  
 916 at nodes. Silhouettes from PhyloPic.org.



918 **Figure 3.** Summary of results with highest posterior probabilities in hominoids (Family Hominoidea).  
 919 Vertebra diagrams and symbols are the same as in Figure 2. Note that this figure supported the results of  
 920 Analysis 1. Analysis 2 supports a  $LCA_{H-P}$  with 6 sacral vertebrae and 30 precaudal vertebrae, but is  
 921 otherwise the same. Silhouettes from PhyloPic.org.

922

923

924 **Table 1**

925

926 Taxa and specimens.

927

Order	Family	Analyses used	Number of Individuals	Number of polymorphisms (Analysis 1)	Number of Polymorphisms (Analysis 2) <sup>a</sup>
Genus & Species					
Rodentia					
	Muridae				
	<i>Rattus norvegicus</i>	1	45	2	N/A
	Dipodidae				
	<i>Jaculus orientalis</i>	1	19	1	N/A
	Castoridae				
	<i>Castor canadensis</i>	1	54	1	N/A
	Heteromyidae				
	<i>Dipodomys ordii</i>	1	17	2	N/A
	Pedetidae				
	<i>Pedetes capensis</i>	1	21	1	N/A
	Sciuridae				
	<i>Tamiasciurus hudsonicus</i>	1	20	2	N/A
	Aplodontidae				
	<i>Aplodontia rufa</i>	1	17	1	N/A
	Chinchillidae				
	<i>Lagostomus maximus</i>	1	11	1	N/A
	Echimyidae				
	<i>Myocastor coypus</i>	1	23	3	N/A
Lagomorpha					
	Leporidae				
	<i>Lepus timidus</i>	1	14	2	N/A
Dermoptera					
	Cynocephalidae				
	<i>Cynocephalus volans</i>	1	16	3	N/A
	<i>Galeopterus variegatus</i>	1	17	4	N/A
Scandentia					
	Tupaïidae				
	<i>Tupaia glis</i>	1	8	1	N/A
	<i>Tupaia minor</i>	1	4	2	N/A
	Ptilocercidae				
	<i>Ptilocercus lowii</i>	1	8	3	N/A
Primates					
	Lorisidae				
	<i>Perodicticus potto</i>	1	45	3	N/A
	<i>Arctocebus calabarensis</i>	1	25	5	N/A
	<i>Nycticebus coucang</i>	1	29	2	N/A

<i>Loris tardigradus</i>	1	19	3	N/A
<i>Loris lydekkerianus</i>	1	6	3	N/A
Galagidae				
<i>Galagoides demidovii</i>	1	12	3	N/A
<i>Otolemur garnettii</i>	1	12	2	N/A
<i>Otolemur crassicaudatus</i>	1	21	1	N/A
<i>Galago moholi</i>	1	5	1	N/A
<i>Galago gallarum</i>	1	6	3	N/A
<i>Galago senegalensis</i>	1	15	1	N/A
<i>Euticus elegantulus</i>	1	53	3	N/A
Daubentonidae				
<i>Daubentonia madagascariensis</i>	1	9	2	N/A
Lemuridae				
<i>Varecia variegata</i>	1	12	1	N/A
<i>Lemur catta</i>	1	14	4	N/A
<i>Hapalemur griseus</i>	1	9	1	N/A
<i>Eulemur mongoz</i>	1	13	2	N/A
<i>Eulemur coronatus</i>	1	4	2	N/A
<i>Eulemur collaris</i>	1	9	2	N/A
<i>Eulemur fulvus</i>	1	12	1	N/A
<i>Eulemur albifrons</i>	1	16	1	N/A
<i>Eulemur rufus</i>	1	6	2	N/A
<i>Eulemur macaco</i>	1	13	2	N/A
Cheirogaelidae				
<i>Cheirogaleus major</i>	1	7	4	N/A
<i>Cheirogaleus medius</i>	1	5	2	N/A
<i>Microcebus murinus</i>	1	9	4	N/A
Lepilemuridae				
<i>Lepilemur ruficaudatus</i>	1	13	1	N/A
Indriidae				
<i>Propithecus diadema</i>	1	9	1	N/A
<i>Propithecus verreauxi</i>	1	10	5	N/A
<i>Avahi laniger</i>	1	12	1	N/A
<i>Indri indri</i>	1	27	3	N/A
<i>Phaner furcifer</i>	1	4	1	N/A
Tarsidae				
<i>Tarsius bancanus</i>	1 and 2	6	1	1
<i>Tarsius tarsier</i>	1	4	1	N/A
Aotidae				
<i>Aotus trivirgatus</i>	1	4	2	N/A
<i>Aotus azarae</i>	1	34	1	N/A
Callitrichidae				
<i>Saguinus midas</i>	1	5	3	N/A
<i>Saguinus oedipus</i>	1 and 2	20	2	2
<i>Leontopithecus rosalia</i>	1	8	3	N/A
<i>Callithrix jacchus</i>	1 and 2	22	1	1
<i>Callimico goeldii</i>	1	8	3	N/A
Cebidae				
<i>Saimiri sciureus</i>	1 and 2	53	2	2

<i>Sapajus apella</i>	1 and 2	38	4	4
<i>Cebus albifrons</i>	1	29	3	N/A
<i>Cebus capucinus</i>	1 and 2	29	3	3
Atelidae				
<i>Lagothrix lagotricha</i>	1 and 2	36	2	2
<i>Lagothrix cana</i>	1	9	6	N/A
<i>Brachyteles arachnoides</i>	1	10	4	N/A
<i>Ateles paniscus</i>	1	16	1	N/A
<i>Ateles belzebuth</i>	1	10	1	N/A
<i>Ateles geoffroyi</i>	1 and 2	16	1	1
<i>Ateles fusciceps</i>	1	7	4	N/A
<i>Alouatta pigra</i>	1	4	2	N/A
<i>Alouatta palliata</i>	1	14	2	N/A
<i>Alouatta caraya</i>	1	4	3	N/A
<i>Alouatta seniculus</i>	1 and 2	25	2	2
Pitheciidae				
<i>Callicebus moloch</i>	1	6	4	N/A
<i>Pithecia pithecia</i>	1	13	3	N/A
<i>Pithecia monachus</i>	1	4	2	N/A
<i>Cacajao calvus</i>	1	5	3	N/A
<i>Cacajao melanocephalus</i>	1	8	3	N/A
Hylobatidae				
<i>Nomascus leucogenys</i>	1 and 2	4	4	16*
<i>Nomascus gabriellae</i>	1 and 2	14	2	8*
<i>Nomascus concolor</i>	1 and 2	25	2	1
<i>Hylobates pileatus</i>	1 and 2	7	3	12*
<i>Hylobates lar</i>	1 and 2	266	2	4
<i>Hylobates muelleri</i>	1 and 2	35	2	6*
<i>Hylobates klossii</i>	1 and 2	12	3	12*
<i>Hylobates moloch</i>	1 and 2	38	2	6*
<i>Hylobates agilis</i>	1 and 2	37	2	8*
<i>Symphalangus syndactylus</i>	1 and 2	98	3	6
<i>Hoolock hoolock</i>	1 and 2	34	2	3
Hominidae				
<i>Pongo pygmaeus</i>	1 and 2	142	2	4
<i>Pongo abelii</i>	1 and 2	48	3	4
<i>Pan troglodytes</i>	1 and 2	525	4	8
<i>Pan paniscus</i>	1 and 2	55	2	3
<i>Homo sapiens</i>	1 and 2	893	2	3
<i>Gorilla gorilla</i>	1 and 2	409	4	5
<i>Gorilla beringei</i>	1 and 2	109	2	2
Cercopitheciidae				
<i>Trachypithecus phayrei</i>	1	23	1	N/A
<i>Trachypithecus obscurus</i>	1	23	2	N/A
<i>Trachypithecus cristatus</i>	1 and 2	118	1	1
<i>Trachypithecus vetulus</i>	1	4	2	N/A
<i>Semnopithecus entellus</i>	1 and 2	18	2	2
<i>Presbytis melalophos</i>	1	19	2	N/A
<i>Presbytis rubicunda</i>	1	5	2	N/A

<i>Pygathrix nemaeus</i>	1	7	1	N/A
<i>Nasalis larvatus</i>	1 and 2	59	1	1
<i>Procolobus verus</i>	1	4	2	N/A
<i>Procolobus badius</i>	1	40	3	N/A
<i>Colobus guereza</i>	1	44	1	N/A
<i>Colobus angolensis</i>	1	9	1	N/A
<i>Macaca sylvanus</i>	1	22	1	N/A
<i>Macaca nemestrina</i>	1	15	2	N/A
<i>Macaca fascicularis</i>	1 and 2	98	2	1
<i>Macaca fuscata</i>	1	884	1	N/A
<i>Macaca mulatta</i>	1	42	2	N/A
<i>Macaca arctoides</i>	1 and 2	29	2	2
<i>Theropithecus gelada</i>	1	32	1	N/A
<i>Papio papio</i>	1	17	3	N/A
<i>Papio hamadryas</i>	1	35	1	N/A
<i>Papio anubis</i>	1 and 2	59	2	2
<i>Papio cynocephalus</i>	1	62	2	N/A
<i>Papio ursinus</i>	1	13	1	N/A
<i>Lophocebus aterrimus</i>	1	21	2	N/A
<i>Mandrillus sphinx</i>	1	31	4	N/A
<i>Mandrillus leucophaeus</i>	1 and 2	20	3	3
<i>Lophocebus albigena</i>	1 and 2	87	1	1
<i>Cercocebus torquatus</i>	1	16	1	N/A
<i>Cercocebus atys</i>	1	13	2	N/A
<i>Cercocebus chrysogaster</i>	1	14	2	N/A
<i>Cercocebus agilis</i>	1	10	2	N/A
<i>Cercopithecus neglectus</i>	1	16	2	N/A
<i>Cercopithecus pogonias</i>	1	24	2	N/A
<i>Cercopithecus mona</i>	1	13	3	N/A
<i>Cercopithecus nictitans</i>	1	22	3	N/A
<i>Cercopithecus mitis</i>	1	28	2	N/A
<i>Cercopithecus ascanius</i>	1	117	3	N/A
<i>Cercopithecus cephus</i>	1	35	2	N/A
<i>Cercopithecus lhoesti</i>	1	9	1	N/A
<i>Erythrocebus patas</i>	1 and 2	35	1	1
<i>Chlorocebus cynosuroides</i>	1	10	1	N/A
<i>Chlorocebus aethiops</i>	1	17	3	N/A
<i>Chlorocebus pygerythrus</i>	1	13	2	N/A
<i>Chlorocebus sabaeus</i>	1	15	1	N/A
<i>Miopithecus talapoin</i>	1 and 2	16	2	2
Total		6216		

N/A = not applicable (i.e., taxon was not used in Analysis 2).

<sup>a</sup> Star (\*) indicates that a uniform prior was included for the caudal count associated with at least one cervical-thoracic-lumbar-sacral formula.

**Table 2**

Summary of selected results of Analysis 1, including full formula and lumbar counts.

Node	Full formulae >5%	Posterior probability (full formula)	Lumbar counts >5%	Posterior probability (lumbar count)	95% highest posterior density for lumbar count
Primates	7C 13T 6L 3S	38.4%	6	67.3%	6–7
	7C 13T 6L 4S	28.3%	7	31.7%	
	7C 12T 7L 3S	15.3%			
	7C 13T 7L 3S	12.1%			
Strepsirrhines	7C 13T 7L 3S	38.8%	7	58.8%	6–8
	7C 13T 6L 4S	16.2%	6	34.0%	
	7C 13T 6L 3S	12.9%	8	6.8%	
	7C 12T 7L 3S	8.3%			
Lorisoids	7C 14T 7L 4S	35.4%	7	78.8%	6–7
	7C 15T 7L 4S	16.7%	6	17.6%	
	7C 14T 7L 5S	7.2%			
	7C 14T 7L 3S	6.2%			
	7C 14T 6L 4S	6.0%			
Galagids	7C 13T 6L 3S	76.8%	6	95.9%	6
	7C 14T 6L 3S	15.9%			
Lemuroids	7C 13T 7L 3S	45.1%	7	64.2%	6–8
	7C 12T 7L 3S	13.0%	6	22.2%	
	7C 12T 8L 3S	11.9%	8	13.4%	
	7C 13T 6L 3S	11.9%			
	7C 13T 6L 4S	8.1%			
Indriids	7C 12T 8L 3S	99.2%	8	99.2%	8
Haplorhines	7C 13T 6L 3S	47.6%	6	70.7%	6–7
	7C 13T 6L 4S	22.0%	7	27.7%	
	7C 12T 7L 3S	15.0%			
	7C 13T 7L 3S	10.0%			
Anthropoids	7C 13T 6L 3S	79.9%	6	83.5%	6–7
	7C 12T 7L 3S	11.9%	7	13.4%	
Platyrrhines	7C 13T 6L 3S	94.5%	6	94.7%	6–7
			7	5.2%	
Atelids	7C 14T 5L 3S	88.8%	5	92.5%	4–5
Atelines	7C 14T 4L 3S	94.7%	4	95.6%	4
Catarrhines	7C 13T 6L 3S	69.2%	6	74.1%	5–7
	7C 12T 7L 3S	17.7%	7	18.2%	
	7C 13T 5L 4S	7.4%	5	7.7%	
Cercopithecoi ds	7C 12T 7L 3S	99.1%	7	99.1%	7

Hominoids	7C 13T 5L 4S	88.8%	5	92.0%	4-5
Hylobatids	7C 13T 5L 4S	97.4%	5	>99.9%	5
Hominids	7C 13T 4L 5S	85.7%	4	92.0%	4-5
			5	6.4%	
Hominines	7C 13T 4L 5S	69.5%	4	89.9%	3-4
	7C 13T 4L 6S	18.4%	3	9.1%	
	7C 13T 3L 6S	9.0%			
<i>Pongo</i>	7C 12T 4L 5S	94.0%	4	>99.9%	4
	7C 12T 4L 6S	5.9%			
<i>Gorilla</i>	7C 13T 3L 6S	85.9%	3	86.0%	3-4
	7C 13T 4L 5S	11.2%	4	14.0%	
<i>Pan-Homo</i>	7C 13T 4L 5S	59.3%	4	96.8%	4
	7C 13T 4L 6S	39.4%			
<i>Pan</i>	7C 13T 4L 6S	77.2%	4	99.6%	4
	7C 13T 4L 5S	22.3%			

Abbreviations: C = cervical vertebra; T = thoracic vertebrae; L = lumbar vertebrae; S = sacral vertebrae.



**Table 3**

Summary of selected results of Analysis 2, including full formula and lumbar counts.

Node	Full formulae >5%	Posterior probability (full formula)	Lumbar counts >5%	Posterior probability (lumbar count)	95% highest posterior density for lumbar count
Hominoids	7C 13T 5L 4S 3Ca	18.1%	5	69.4%	4–6
	7C 13T 5L 4S 4Ca	16.9%	4	19.0%	
	7C 13T 5L 5S 3Ca	15.3%	6	11.2%	
	7C 13T 4L 5S 3Ca	7.4%			
Hylobatids	7C 13T 5L 4S 3Ca	67.4%	5	99.7%	5
	7C 13T 5L 4S 2Ca	11.0%			
	7C 13T 5L 5S 3Ca	10.3%			
	7C 13T 5L 5S 2Ca	6.9%			
Hominids	7C 13T 4L 5S 3Ca	26.5%	4	75.7%	4–5
	7C 13T 4L 6S 3Ca	20.9%	5	20.8%	
	7C 13T 4L 5S 4Ca	9.7%			
	7C 13T 5L 5S 3Ca	5.7%			
	7C 12T 5L 5S 3Ca	5.4%			
	7C 12T 4L 6S 3Ca	5.1%			
Hominines	7C 13T 4L 6S 3Ca	39.8%	4	85.0%	3–5
	7C 13T 4L 5S 3Ca	16.7%	3	8.4%	
	7C 13T 4L 5S 4Ca	9.6%	5	6.6%	
	7C 13T 4L 6S 2Ca	6.5%			
	7C 13T 3L 6S 3Ca	5.1%			
<i>Pongo</i>	7C 12T 4L 5S 3Ca	62.9%	4	99.8%	4
	7C 12T 4L 6S 3Ca	24.1%			
	7C 12T 4L 6S 2Ca	10.3%			
<i>Gorilla</i>	7C 13T 3L 6S 2Ca	39.7%	3	63.1%	3–4
	7C 13T 4L 6S 3Ca	29.9%	4	36.9%	
	7C 13T 3L 6S 3Ca	15.2%			
	7C 13T 3L 6S 4Ca	8.1%			
<i>Homo-Pan</i>	7C 13T 4L 6S 3Ca	42.6%	4	89.2%	4–5
	7C 13T 4L 5S 4Ca	14.0%	5	8.9%	
	7C 13T 4L 6S 4Ca	11.5%			
	7C 13T 4L 5S 3Ca	11.0%			
	7C 13T 4L 6S 2Ca	5.2%			
<i>Pan</i>	7C 13T 4L 6S 3Ca	53.1%	4	98.0%	4
	7C 13T 4L 6S 4Ca	21.0%			
	7C 13T 4L 6S 2Ca	11.5%			
	7C 13T 4L 5S 3Ca	6.5%			
	7C 13T 4L 5S 4Ca	5.6%			

Abbreviations: C = cervical vertebra; T = thoracic vertebrae; L = lumbar vertebrae; S = sacral vertebrae; Ca = caudal (or coccygeal) vertebrae